Title	FIELD-EXPERIMENTAL STUDY OF SHEAR WAVE AND THE RELATED PROBLEMS
Author(s)	KITSUNEZAKI, Choro
Citation	Contributions of the Geophysical Institute, Kyoto University (1971), 11: 103-177
Issue Date	1971-12
URL	http://hdl.handle.net/2433/178596
Right	
Type	Departmental Bulletin Paper
Textversion	publisher

Kyoto University

FIELD-EXPERIMENTAL STUDY OF SHEAR WAVES AND THE RELATED PROBLEMS

Chōrō KITSUNEZAKI

Abstract

The author has been engaged in field-experimental studies of S waves since 1957. In this paper, he discusses fundamental aspects of the S wave from field-experimental point of view, giving systematic form to his previous works.

In an earlier part of this paper, problems of detection and generation of S waves are discussed, and they are connected to the methods of S wave logging in the later part. Significance of tube wave velocity and resistivity logging are emphasized as an indirect method of S wave logging. Results of experiments suggest that both are favourable for the purpose of S wave logging. From the resistivity logs void ratios are deduced, and the relation between S wave velocity and void ratio are compared with Hardin's relations obtained by laboratory experiments. Both agree in the main essentials. Velocity variation of weathered granite, obtained in field experiment, is dicussed in connection with sample tests by other authors. Empirical relations between P and S wave velocities are presented to the system covering granular soil and siliceous rock.

In the final section, significance and methods of S wave logging are discussed in connection with earthquake engineering.

Contents

List of symbols

symbol	explanation	Section
a	(as suffix) acceleration	6–1
a	radius of source sphere	4–2
A	constant	8–2

A	vector potential	4
b	radius of borehole	4–2
b	radius of contact area	3–3
B	(as suffix, etc.) tube wave	8–1
B	(as suffix) rock block	3–3
c	coefficient	3–3
C	proportion constant	9–2
C	capacitance	8–1
d	diameter of borehole	8–1
e	base of natural logarithm	
E	(as suffix) elasticity of media	3–3
E	Young's modulus	3–3
f	frequency	
F	force	4, 9–4
$g(t)$	wave form of source	4
G	magnitude of source force	4
h	a half of interval of source points	4
h	damping constant	3–3, 4–4
i	(as suffix) mud invasion	8–2
j	$\sqrt{-1}$	
K	unit vector along z axis	4–1
k	V_B/V_S	3–5, 8–1
K	stiffness	3–3, 4–4
m	(as suffix) mud water	8–2
m	mass of source plate	4–4
M	mass of a hammer as source	4–4
M	mass of a geophone body	3–4
N	number	3–4
O	origin of coordinate	
p	pressure due to wave signal	3–5
P	(as suffix etc.) P wave	
P	magnitude of source pressure	4
P	effective pressure	8, 9
r	radial distance	4, 6
R	resistivity	8–2
R	coefficient of liquid-like friction	3, 4–4
R	(as suffix) rubber tube	3–4
R	(as suffix) radiation	4–4
S	(as suffix etc.) S wave	
SV	(as suffix etc.) SV wave	
SH	(as suffix etc.) SH wave	
t	time	

u	displacement	
v	(as suffix) particle velocity	6–1
V	propagation velocity	
w	(as suffix) water	
x	distance	6–1
x, y, z	axes of rectangular coordinate	
α	attenuation constant	6
β	elasticity of borehole wall	8–1
$\delta\,(t)$	δ function	6
γ	V_P/V_S	
ρ	density of medium	
κ	bulk modulus	8–1
μ	rigidity	
θ	μ'/μ	6–1
θ	angle measured from z axis	
ϕ	porosity	8, 9
ϕ	scalar potential	4
ψ	azimuth (longitude) measured from x coordinate	4
σ	Poisson's ratio	3, 4
$\varLambda$	wavelength	
λ	Lame's contant	
ν	constant	8–2
ω	angular frequency	
χ	volumetric strain	4
$\tilde{\omega}$	rotation vector	4
" $\cdot$ "	time derivative of first order	
" $\cdot\cdot$ "	time derivative of second order	

1. Introduction

(1) Historical review

In the field of natural earthquake, seismologists have been very familiar with the shear (S) wave as well as the P wave and the surface waves. Further back in the history of seismic prospecting, certain seismologists naturally approached detection of the shear wave, but they seem to have been too hasty in identification of the S wave, compared with existing knowledge of real soils and instrumental development at that time. (Nasu et al. [1936])

In these several ten years, seismic prospecting however has been mainly developed in the field of oil prospecting, and the P wave alone has been used for oil prospecting. Dynamite explosion has been popular as the powerful energy source. It has been thought that the S wave can be hardly generated by an explosion.

For the above reasons, utility of the S wave had been ignored before these ten years except for a few researchers.

More than ten years ago the author found the generation of the S wave by a small explosion in the course of the experiments in the mine drifts as to a seismic prospecting (Kitsunezaki [1960b]). The same kind of experiment had been reported by Linsser [1955]. Since then the author has been concerned improving the detection of the S wave and its application.

Independent of this nearly at the same time, some seismologists wanted to know real rigidity of the near ground surface, in order to compare results of wave experiments in field with theoretical calculations. The Seismic Exploration Group of Japan carried out some experiments for the generation of the S wave (for example, Kobayashi [1959]). Based on the works of this group, such a practical method becomes popular in Japan that a wooden plate pressed on the ground surface is struck by a hammer and the SH wave is generated. The idea is principally the same as Jolly's experiment [1956]. The method is usually called "ita-tataki" in Japanese that means striking a wooden plate.

Very recently an earnest interest regarding application of the S wave has been expressed in some fields of civil engineering. One of them is related to soil mechanics and rock mechanics. Determination of elastic moduli applied to design of structures is of course an important problem. In connection with *in situ* survey of ground condition, the relations of shear wave velocity with strength (including standard penetration test value) and state of weathering and fracturing have been studied (Kitsunezaki [1965], Yoshikawa and Kitsunezaki [1966], Yoshikawa and Zako [1970]). Detailed discussions about these problems are beyond the subject of this paper.

Another important application can be found in engineeing seismology. Distribution of shear wave velocity and its attenuation constant are main factors to estimate ground characteristics for earthquake vibration. So, in some regions of Japan, systematic measurement of the shear wave has been started in order to build effective plan to prevent disasters due to earthquakes (Shima et al. [1968], for example). These problems on the earthquake engineering will be discussed in the end of this paper.

(2) *Approach in this paper*

One of the conclusions in the author's experience is that the generation of the shear wave itself is not so uncommon phenomenon, even in relatively usual methods of seismic prospecting. The author's main effort has been to further improvement of detecting techniques for the S wave.

In connection with the S wave detection, fundamental properties of the wave will be introduced in Section 2.

In Section 3, instrumental problems on detection of the S wave will be discussed.

Section 4, problems on shear wave sources will be discussed from practical

point of view. Sometimes, some useful informations as to S wave properties of the ground are supplied not only by the waves generated directly from the source but by the S wave converted from P wave at a particular boundary layer. This problem will be discussed in Section **5.**

The author's study started from high frequency seismic experiments in mine drifts. His continuous interest in detailed survey of the structure (by using seismic waves of short wavelength) has been kept in the author's study. Problems on wavelength and frequency will be also considered in Section **3** and **4** from practical point of view. Some problems on attenuation of the wave amplitude are discussed in Section **6.**

For detailed and exact investigation of the S wave in field, logging technique becomes important. The author will discuss this problem in Section 7 from general point of view.

In the following description, "direct S wave logging" is used as the word to mean that the S wave is directly measured in bore holes. Sometimes direct S wave logging is difficult to be carried out in real field conditions. It is also necessary to develop some other techniques estimating S wave velocity from the result of other logging which is easier than the direct logging in practice. Such a technique is called an "indirect logging" in this paper. Two methods of indirect logging are proposed in Section **8.**

Based on results of the S wave experiments in the field, some characteristics regarding S and P wave velocity in natural earth material will be demonstrated in Section **9.**

2.   Characteristics and identification of shear wave

2–1   Characteristics of S wave

Well-known equation of motion of elastic medium can be expressed as follows,

$$\rho \frac{\partial^2 u}{\partial t^2} = (\lambda + 2\mu) \, \nabla (\nabla u) - \mu \nabla \times \nabla \times u \tag{2–1}$$

where u is displacement vector of a particle in the medium. λ and μ are Lame's constants. Vector u can be written as summation of two vectors, u_P and u_S, which has scalar potential, ϕ, and vector potential, A, respectively. That is,

$$\left. \begin{aligned} u &= u_P + u_S \\ u_P &= \nabla \phi, \quad u_S = \nabla \times A \end{aligned} \right\} \tag{2–2}$$

and then

$$\left. \begin{aligned} \chi &\equiv \nabla u = \nabla u_P \\ \tilde{\omega} &\equiv \nabla \times u = \nabla \times u_S \end{aligned} \right\} \tag{2–3}$$

Substituting Eq. (2–3) into Eq. (2–1), we get two independent equations,

$$\frac{\partial^2 \chi}{\partial t^2} = V_P{}^2 \, \nabla^2 \, \chi$$

$$\frac{\partial^2 \tilde{\omega}}{\partial t^2} = V_S{}^2 \, \nabla^2 \, \tilde{\omega}$$

$$(2\text{--}4)$$

where

$$V_P = \sqrt{(\lambda + 2\mu)/\rho}$$

$$V_S = \sqrt{\mu/\rho}$$

$$(2\text{--}5)$$

χ means volumetric strain of an element of the medium, $\tilde{\omega}$ denotes rotation vector of u.

From the above relations, well-known characteristics of the shear wave are introduced as follows;

(*Character a*) As to the S wave (displacement: u_S, propagation velocity: V_S),

$$\tilde{\omega} \neq 0, \quad A \neq 0 \text{ and } \chi = 0, \quad \phi = 0.$$

Compared with this, the P wave (displacement: u_P, propagation velocity: V_P) has the contrary characters; $\tilde{\omega} = 0$, $A = 0$ and $\chi \neq 0$, $\phi \neq 0$. These are the essential characters defining the S wave.

If u is the displacement of the waves (plane wave) propagating along x direction in cartesian coordinate, u_P and u_S show the following characters.

(*Character b*) As to the S wave, a particle moves in the direction perpendicular to the propagation direction, that is, $u_S \perp x$. As to the P wave, a particle moves along the propagation direction, that is, $u_P // x$.

This is an important character of the S wave, but this cannot be kept in general propagation, for example, the spherical wave, in strict meaning. Also in spherical propagation, however, at the distance several wave lengths apart from the wave source point, the waves have approximately the characters of plane wave (see Section 4).

(*Character c*) The S wave is the so called body wave as well as the P wave. If the particular boundaries exist, the surface waves may exist. The body waves can be distinguished from the surface waves, by the nature of the former not showing considerable decrease of amplitude at distance more than several wave lengths apart from the boundary.

2–2 Identification of S wave

(*1*) *Rotation seismometer* Rotation of a medium element is one of the most essential character of the S wave. Some trials to detect the rotation have been done by the investigators (Hagiwara [1958], Tazime [1965]). Although favourable results are reported in the experiments in laboratory and under selected field conditions, the reliable rotation seismometers have not been obtained. Difficulties of putting

the rotation seismometer in practice were noted by the author (Kitsunezaki [1971b]).

Generally speaking in order to measure some quantities as to motion of body, it is necessary to compare the body with the scale (coordinate) which does not move (the first type of the scale) or move in such a simple principle as can be estimated from the measured value (the second type of the scale). In natural or artificial earthquake, any points surrounding the point to be measured may move, that is, we can not get the first type of the scale, so we use a pendulum system as the second type of the scale. This condition is the same in detection of rotational movement as displacing movement (usual seismometer and geophone).

Very small discrepancy of the gravity center of pendulum from rotation axis carries considerable error in output by reacting acceleration of displacing motion. The author believes that it is very difficult to make the reliable rotation seismometer for practical use in field conditions, by our usual technique. At seismological observatories, however, where the instruments can be carefully maintained in favourable constant condition, we may have the reliable rotation seismometer.

Regarding practical use of the rotationseismometer in general field conditions, there is also another difficulty. Rotation has the same kind of character as strain which is the derivative of displacement as to distance. In practical measurement, difference of the displacement at two neighbouring points is detected. Random inhomogeneity of media being usual in field will disturb such a quantum as strain more severely than as displacement.

By the reason discussed above, the author has not made effort to detect rotation. (2) As to "*Character (a)*" of the S wave, there is another property, that is, $\chi=0$. (potentials A and ϕ can not be objective to be measured directly.) χ is also a kind of strain. Design of a portable detector to measure this completely is difficult. It can, however, be somewhat realized by using hydrophones. The problems regarding this will be discussed in the following section.

After all, "*Character (b)*" becomes important for practical detection of the S wave. To bring this in practice, usual velocity type geophones and the composite geophones, in which three components of them are set mutually in rectangle, can be used.

In usual field experiments, propagation and vibration direction of the waves can be presumed, at least roughly. So, $u_s \perp x$ in "*Character (b)*" can be an effective criterion in identification of the S wave.

Test as to "*Character (c)*" can be put in practice by carrying out observation in bore holes and drifts.* "*Character (c)*" and the property, $\chi=0$, are used as sup-

---

* $A/d < 1.5$ is the condition for existance of the axial symmetrical surface wave propagating along a cylindrical hole in infinite (homogeneous and isotropic) media, where A is wavelength of the wave and d is diameter of the hole (Biot [1952], Ewing et al [1957]). The corresponding value may be smaller for nonsymmetrical waves than the above. Hence, if $A > 1.5d$ is assured for observed waves, they are not the surface waves along borehole. In the above explanation, the surface wave of Stoneley type is excluded. This corresponds to the tube wave explained in Section 8. Tube wave can be easily identified by its velocity characteristics. (Its velocity is usually lower than velocity of liquid contained in the hole.)

plementary criteria to the criteria, $u_s \perp x$.

3. Instrument and detection

3-1 Recording system

The author's recording systems for the experiments consist of detectors (geophones), an amplifing equipment and an electromagnetic recorder with galvanometers, as well as the conventional seismic equipment. Amplifier outputs were sometimes delivered to a magnetic recorder simultaneously with the electromagnetic recorder, at earlier experiments in mine drifts.

Three kinds of systems combining of an amplifing equipment and an electromagnetic recorder have been used.

(a) The vacuum tube amplifier (6 elements) specially designed by the author was used with combination of high paper-speed recorder (maximum: 4 m/sec) for measurement of high frequency seismic waves in mine drift (Kitsunezaki [1960 a]). An amplifier unit has flat transfer characteristics (amplification factor) in about 50–5000cps and equips high-cut and low-cut multi-filters. Natural frequency of the galvanometer used is 1000–5000cps. Usually, 5000cps ones were used. In this case we can expect about 2000cps as the highest frequency limit of the flat characteristics. The real model of the amplifier was changed several times. Equipments of this type were designed and used in 1957–1962.

(b) The twelve elements transistor amplifier, constructed by a company to the author's special order, was combinated with a standard electromagnetic recorder, of which maximum paper speed is 1 m/sec. The frequency characteristics of the amplifier unit is nearly the same as that of the system (a). Natural frequency of the galvanometer is 500–2000cps. Usually 500cps ones were used. In this case the highest frequency limit of the flat characteristics is about 200cps. This type has been used since 1964 (Kitsunezaki [1965]).

(c) This is a combination of usual commercial amplifier for seismic prospecting (refraction type, flat characteristics: 5–1000cps (more than)) and an electromagnetic recorder which is the same as that of system (b). Through the whole period of the author's experiment, this system has been used due to its convenience when considerably high frequency recording was not necessary.

The system (a) and (b) can be used with a magnetic recorder. In the experiments described in this paper, magnetic recorder was used only in the system (a).

3-2 Detector problems

(1) Frequency range and geophones applicable

The field experiments discussed in this paper are on a relatively small scale. The wavelength of the seismic waves detected is 0.2–20m. The frequency of the wave is 100–3000cps in hard rocks, and 30–300cps in unconsolidated soils, except

where particularly small scale measurement is carried out in boreholes for velocity logging.

For normal experiments practised in unconsolidated soils, we can use usual commercial geophones without important difficulties. Generally, however, it is convenient to use the proper type of detector by which vibration of any direction can be detected (used as a vertical detector or horizontal one in common). Due to the above consideration, 25–28cps (natural frequency) moving coil type geophones have been used. In rocks and soils of special case higher frequency characteristics of the detector becomes important for exact detection of the vibration.

The most important factor governing the higher frequency characteristics is the secondary resonance of pendulum system of detector. On the frequency range beyond the secondary resonance, many resonances and anti-resonances of the higher mode appear, and calibrated measurement becomes difficult. In general, ratio of the secondary resonance frequency to the fundamental one (natural frequency of usual sense) is decided by the ratio of mass of the pendulum to that of spring (Kitsunezaki [1971 a]).

By reason of the above, in order to assure wide frequency range applicable, excellent design becomes necessary as to the pendulum system. And the higher natural frequency becomes needed for the geophones to assure exact detection of the higher frequency vibration. Usual commercial geophones do not always satisfy the necessary characteristics, because they are designed to be applicable in the usual frequency range up to about 100cps. For example, one type (natural frequency: 14cps) of commercial geophones showed the characteristics having resonance at 700–800cps (Kitsunezaki [1960]). (See Fig. 3–1.)

At an earlier period of the experiment, the high frequency geophones (natural frequency: 100cps, oil damping), which were specially designed by a company based on the author's order, were used for the work in mine drifts (Kitsunezaki [1960]). At a relatively later period of the experiment, some types of usual commercial geophone with the natural frequency of 25–28cps are used (NEC VP202, NEC VP425, GEO SPACE HS-J-K28).

In general, complete calibration of the geophones in the higher frequency range had been difficult, before the author developed the particular method which will be explained in the following item. At an earlier time, reliable tests with a vibration table were carried out in the restricted frequency range up to about 100cps, and beyond the above the supplementary tests were put in practice by measuring electric impedance of the circuit including pendulum system in free condition (Kitsunezaki [1964]). And after all, it was applied as a practical criteria for assuring the normal high frequency characteristics that the geophones set firmly in rock did not show resonance-like vibration but simple wave form on the record as response for the wave radiated from the simple small source (Fig. 3–1). For the whole kinds of the geophones used, the applicable frequency ranges were decided by the above method from practical point of view. The discussions about the wave in the following section are
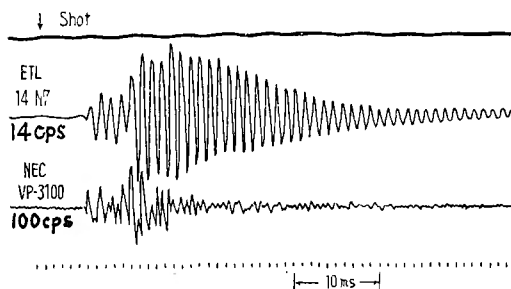
Fig. 3–1. A record comparing responses of two models of
geophone for the same input signal. The upper trace shows
predominant resonance of the second mode. (Cited from
Kitsunezaki et al. [1960].)

based on the measurements in such an applicable frequency range at least.

(2) *Complete calibration in higher frequency range*

Several years ago, the author [1967] was sucessful in calibrating the higher
frequency characteristics of the geophone by the following method.

A geophone to be tested is fixed at an end of an elastic bar, and its response for
the wave pulse, generated by impulsion at another end, is displayed on the tube of
synchroscope. Simultaneously with this, particle velocity (input) of the geophone
is detected by recording the response of a pair of strain gauges adhered at proper
position of the bar. Complete frequency characteristics can be obtained by com-
paring the both responses analytically. In this method, it is most important point
that one dimensional wave pulse, which can be exactly detected by the strain gauges,
is used as an input signal instead of usual mechanical vibration.

By applying the above method a model of commercial geophones (GEO SPACE
HS-J-K28cps) was calibrated in the frequency range up tp 3000cps and was assured
to react without considerable difficulties in this frequency range. Hence, this model
of geophone is applied to recent experiments in higher frequency range.

3–3 Installation of geophone

The installations of geophones needs careful consideration in order to get reliable
records of higher frequency waves. The S wave usually appears on a record as a
later phase, following the P wave. Hence, identification of the S wave requires ex-
cellent quality of record through the whole wave train. Excellant and careful tech-
niques are needed even for the detection of its travel time. This is the very point
which is different from the corresponding case of the P wave. Regarding installation
of geophones, there are two problems. One of them is installation of the geophones
themselves and the other is the condition of the site where the geophones are installed.
Two problems are the same from the physical point of view. As to the detection of
the waves with a geophone, it is principally presupposed that motion of the geophone
body completely follows that of the point in medium to be measured. The main

point of geophone installation is to assure this.

(1)   Contact stiffness, K

Incomplete installation of a geophone body can be expressed as such a model as a sort of elastic compliance exists between the geophone body and the medium. This idea is illustrated in Fig. 3-1. Transfer characteristics from vibration $(\dot{u}')$* of the medium to that $(\dot{v})$ of the geophone body shows such a high cut characteristic that the resonance frequency resulted from combination of the compliance $(1/K)$ and mass (M) of the geophone body is the cut frequency (f_0).

$$\omega_0 \equiv 2\pi f_0 = \sqrt{K/M} \qquad (3\text{-}1)$$

f_0 gives a measure for the highest limit of the wave frequency to be detected normally. Regarding the stiffness, K, two causes should be considered. One (Kc) is due to real incompleteness of fixing the geophone on the ground, that is, the contact area between geophone and the ground is small, or the cementing material is soft. Characteristics due to this can be improved by careful fixing. Another (K_E) is due to elasticity of media itself. The elastic media near the area loaded behaves as an elastic spring system with damper in general. Both spring, K_C and K_E can be thought to be connected in series. K_E, therefore, is the stifiness for the limited case when the contact is complete.
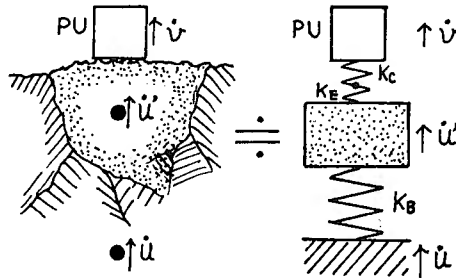

Fig. 3-2.   A model illustrating installation condition of a geophone.

On the plane boundary of semi-infinite solid such a compliance can be deduct from Boussinesq's solution (Love [1952], Timoshenko [1951]). For example, if a load area is circular plane, the stiffness, K_E, is expressed as follows, (suffix "E" omitted)

$$K_\perp \equiv \frac{F_\perp}{v_\perp} = \frac{cbE}{1-\sigma^2} = 4c\,(1-\gamma^{-2})\,\rho\,V_s^2\,b, \qquad (3\text{-}2)**$$

$$c \equiv 3\pi^2/32 = 0.93, \quad \gamma \equiv V_p/V_s,$$

---

* The symbol " · " means time derivative of first order. Hence, $\dot{u}$ means particle velocity (u is displacement).

** 1) It is presupposed for deduction of Eq. (3-2) and Eq. (3-3) that stress over the loaded

for normal force,

$$K_{//} = \frac{F_{//}}{v_{//}} = \frac{K_\perp}{1+0.55B}$$ (3–3)*

$$B = \lambda/(\lambda+2\mu) = 1-2\gamma^{-2}$$

for tangential force.

$E=$Young's modulus, λ and $\mu=$Lame's constants, $\sigma=$Poisson's ratio, $b=$diameter of the circular plane. $F_\perp$ and $F_{//}$ are total force in normal and tangential direction over the loaded area respectively.

On ordinary rock, K_E is large enough for its effect to be discounted. On unconsolidated soil, however, the value of K_E may restrict the highest limit of the frequency of the vibration detected normally. The problem on this will be discussed with problems on the borehole geophone.

After all, regarding the experiments in drifts, rigid bases of geophones were fixed into drill holes with cement in order to assure the complete installation as to K_C (Kitsunezaki [1960 b]).

(2) *Problems on geophone site*

The surface of usual media is disturbed by weathering and fracturing more or less. Also in drifts we can not get ideal states of media, because the surface is usually disturbed by loosening. A block of rock isolated by fissures behaves as if it is a pendulum system consisting of a mass (a rock block) and a spring (contacts at fissure surfaces). As well as the preceeding discussion, a sort of high cut filter characterized by the resonance frequencies exists as to vibration transmission from the surrounding media $(\dot{u})$ to the rock block $(\dot{u}')$.

Therefore, two kinds of filtering (resonance) effect should be considered regarding geophone installation, that is, $\dot{u}'/\dot{u}$ and $\dot{v}/\dot{u}'$. Response as to several kinds of installation for the same input signal are compared in Fig. 3–3(a). From this we can know that the cement fixing prevents the response from high frequency resonance-like oscillation (about 1KC), and that the response is more improved by the installation at hole bottom, where the surface disturbance is lessens.

---

area is uniform (constant). $u_\perp$ and $u_{//}$ are average of displacement in the loaded area. The preassumption, that displacement is uniform in loaded area, is more appropriate for contact of rigid mass, but the analysis becomes complicated. Difference of evaluated results ($K_\perp$ and K) in both cases may be sufficiently small.

2) In Timoshenko's textbook, calculation process for deduction of $K_\perp$ is shown almost completely. $K_{//}$ can be deducted from Love's expression [1952] for displacement due to tangential point force, following the calculation process of $K_\perp$ mentioned above.

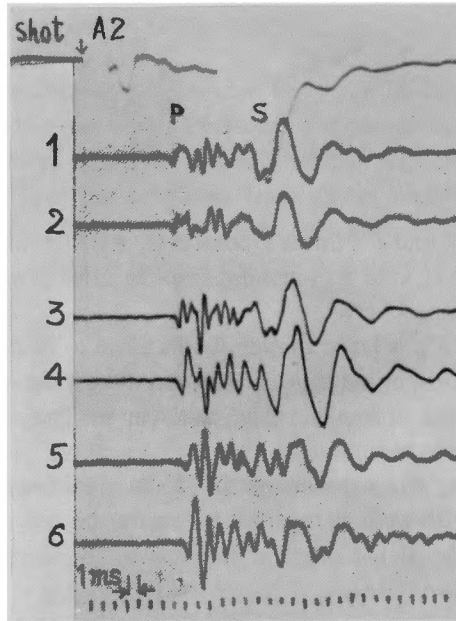3) Erros involved in author's previous report [1970b] has been corrected in these formulae.

Fig. 3–3(a). Comparing responses for several kinds
of installation (geophones : VP–3100 (natural
frequency 100 cps))

trace 1–3   fixed with cement at the bottom of a
             drill hole (1.5m depth).
trace 4   fixed with cement on the wall (rock)
             surface,
trace 5   fixed with wooden wedge on the wall
             (rock) surface,
trace 6   fixed with clay on the wall (rock)
             surface.
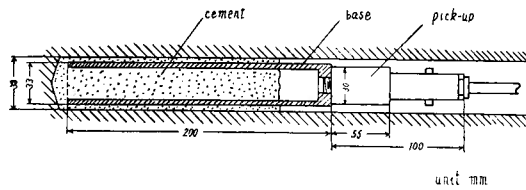
Fig. 3–3(b). Schematic explanation of installation condition
of trace 1–3 in Fig. 3–3(a).

3–4 Clamped borehole geophone

Based on the experiments in drifts, the author believes that the exact detection
of higher frequency waves should be done in boreholes, where the infavourable
surface effect may be reduced, because scale of the disturbed zone near the wall
surface is the same order as the hole diameter. This would be also favourable for

detailed measurement of medium properties (logging). Several kinds of borehole geophones (clamped in holes) had been developed before the author's study (Jolly [1953], McDonal et al. [1958], Halperin et al. [1961]). After some trials had been carried out, the clamp system illustrated in Fig. 3–4 was developed by the author. Expansion of the rubber tube due to water pressure presses the geophone body on the hole wall with the other side where the expansion of the rubber tube is prevented by a rigid back plate. The back plate covers over the tube and is fixed on the geophone body rigidly. Clamp mechanism of this type is almost safely applicable to soft soils. This is the merit of this mechanism, compared with other types.
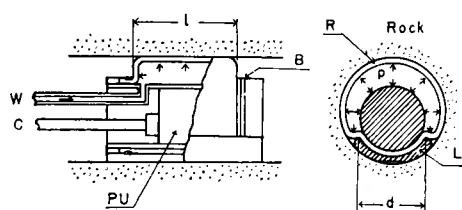

Fig. 3–4(a). Illustration of the clamp system of the borehole geophone.
    R : rubber tube, B : binding wire
  PU : geophone elements (3 components)
    L : rigid back plate
    C : output cable
    W : rubber pipe conducting water
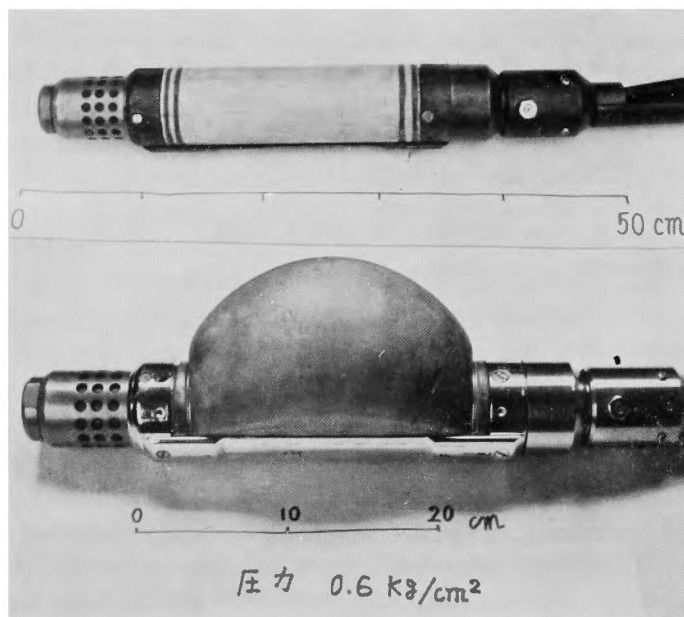   P : water pressure

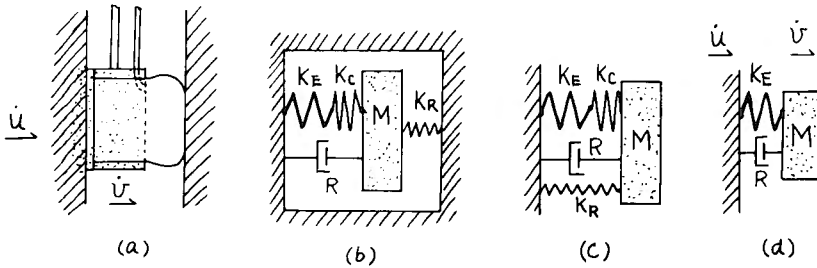Fig. 3–4(b). Photographic view of a model of the borehole geophone.

Fig. 3–5.   Models for installation condition of a clamped borehole geophone.

In Fig. 3–5, effective factors deciding installation characteristics are demonstrated. Definition of notation, K_E, K_C and M, are the same as those in the preceeding discussion. R is a viscoelastic constant expressing damping property of the resonance system due to radiation of the waves and nonelastic property of materials near the contact. K_R is stiffness constant of rubber tube. The model is simplified from (a) to (d) through (b) and (c). Usually K_R K_C, K_R K_E. Effect of K_R, therefore, is omitted. In complete contact state K_E alone is effective as shown in (d).

In such a soft medium as clay and sand, the complete contact above mentioned can be assured by pressing the geophone body effectively. In such a hard medium as rock, K_C may be more effective than K_E.

In the following discussion, the system as shown in Fig. 3–5(d) is assumed to be applicable. If the geophone body contacts with circular contact planes (diameter: b, numbers: N), the resonance frequency of normal vibration is as follows,

$$f_{0\perp} = \frac{1}{2\pi} \sqrt{\frac{NK_E}{M}} = \frac{\sqrt{c(1-r^{-2})}}{\pi} \sqrt{\frac{\rho bN}{M}} \; V_s \doteqdot \frac{V_s}{\pi} \sqrt{\frac{\rho bN}{M}} \qquad (3\text{--}4)$$

For tangential vibration,

$$f_{0/\!/} = (1+0.55B)^{-1/2} f_{0\perp} \doteqdot f_{0\perp} \qquad (3\text{--}5)$$

There are not considerable difference between $f_{0/\!/}$ and $f_{0\perp}$. If the wavelength of the S wave corresponding to f_0 is denoted l_0.

$$\left. \begin{array}{l} l_{0\perp} = \dfrac{\pi}{\sqrt{c(1-r^{-2})}} \sqrt{\dfrac{M}{\rho bN}} \doteqdot \pi \sqrt{\dfrac{M}{\rho bN}} \\[3mm] l_{0/\!/} \doteqdot l_0 \end{array} \right\} \qquad (3\text{--}6)$$

These relations conduct interesting conclusion regarding the highest limit (f_0) of the frequency range to permit normal detection, which is brought by the contact effect: i.e. if it is expressed by the corresponding wavelength (shortest limit) of the S wave, this (l_0) does not practically depend on elastic properties of media, but characteristics of the geophone body, those are, M, b and N. (ρ is assumed to be constant practically.) However very different impression from the above will be

borne as to frequency.

As to the above characteristics, two examples will be shown.

a) The geophone (Fig. 3–4(b)) used at the experiment of 1967 (cited in Section 4, Fig. 4–3).

$M \doteq 4500g$, $\quad b \doteq 2cm$, $\quad N = 4$, $\quad \rho = 2g/cm^3$ (assumed), $\quad \lambda_0 \doteq 53cm$

b) The geophone (Fig. 4–8(b)) used at the experiment of 1968–1969 as to logging source of the S wave (cited in Section 4, Fig. 4–10, 11).

$M \doteq 700g$, $\quad b \doteq 1.5cm$. $\quad N = 4$, $\quad \lambda_0 = 21cm$

In general, characteristics as to the seismic waves can be understood in simple principle by considering the wave length. This fact will be shown also as to other characteristics.

3–5 Detection by means of hydrophone

(*1*) One of the important merits of a hydrophone is that it does not need any rigid installation. Normal detecting can be assured by hanging it freely in water of a borehole. It makes exact detection of higher frequency waves easy. Therefore, installation characteristics of a geophone can be tested by comparing response of it with that of a hydrophone. White [1962] discussed this problem as to an experimental study of attenuation in Pierre Shale. The problems will be discussed again in (3).

(*2*) A hydrophone in a borehole reacts not only to the P wave but to the S wave, though the transfer characteristis depend on incident angle of the waves measured from the hole axis (z). To the SV wave propagating in parallel or in normal direction, the hydrophone does not react. And then, to the SH wave propagating in any incident angle, the hydrophone does not react completely.

In the above description, the hole axis is assumed as vertical (z axis). Therefore, SV and SH are defined as the following. As to SV wave, particle motion is parallel to the plane including the hole axis. As to SH wave, particle motion is perpendicular to the hole axis (horizontal).

The hydrophone characteristics mentioned above can be applied to two purposes. The fact that it does not react to SV wave with particular incident angle as well as SH wave, can be used as useful criterion for identification of the S wave.

Considering these properties and the character mentioned in (*1*), the borehole geophone designed by the author is usually made as a combination of velocity type detectors (3 elements) and a hydrophone. (Saturate gate type magnetic detector is also sometimes installed in the geophone body for supplementary purpose to detect geographical azimuth.) The characteristic, that the hydrophone reacts to SV wave, sometimes provides easy detection of the S wave.

(*3*) White analyzed pressure signals in borehole (infinite length) induced by incidence of seismic waves (plane wave). Ratio of pressure signal (*p*) in water to particle velocity of incident wave is given by the following equation after slight modification as to White's original formula.

$$\frac{p}{\dot{u}_P} = k^2 \, \rho_w \, V_S \, r \, \frac{1 - 2r^{-2} \cos^2\theta}{1 - k^2 \, r^{-2} \cos^2\theta} \tag{3-7}$$

$$\frac{p}{\dot{u}_{SV}} = k^2 \, \rho_w \, V_S \, \frac{\sin 2\theta}{1 - k^2 \cos^2\theta} \tag{3-8}$$

where

$\dot{u}_P$ = particle velocity of P wave

$\dot{u}_{SV}$ = particle velocity of SV wave

θ = incident angle to hole axis

ρ_w = density of water in the hole

V_B = tube wave velocity
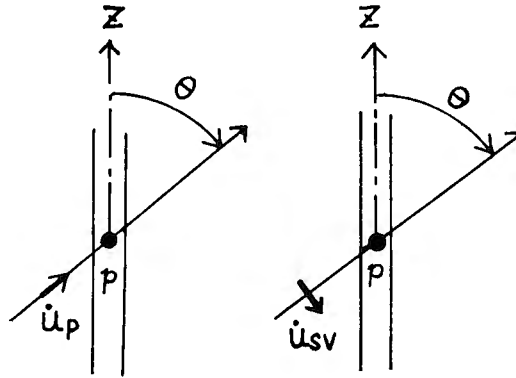
$k = V_B/V_S$, $r = V_P/V_S$

Fig. 3-6.   Illustration showing the waves incident to borehole.
$\dot{u}_P$ and $\dot{u}_{SV}$: particle velocity, p : pressure signal

Results of numerical calculation as to the above relation are shown in Fig. 3-7. The relations are symmetrical as to hole axis.

As discussed in Section 8, experimental results show that value of k^2 is about 0.6 in usual soils. In this case ratio of $p/\dot{u}_{SV}$ to $p/\dot{u}_P$ is about $1.5V_S/V_P$ as to their maximum values. If V_P/V_S ($=r$) is sufficiently larger than unity, $p/\dot{u}_P$, becomes symmetrical to any direction. Of course, a hydrophone reacts to p, and a geophone (velocity type detector) to $\dot{u}$. If response characteristics of both to p and $\dot{u}_P$ respectively are the same in effective frequency range of input signal, wave form of both response must be the same. This has been used as an useful criterion to check installation condition of the geophone body as mentioned in (1).

Fig. 4-3 shows an example of record obtained by the borehole geophone shown in Fig. 3-4 (b), in which a hydrophone and velocity type detectors have practically same (flat) characteristics in the frequency range of 30-200cps. Wave form of both are very similar as to the P wave. In this case geophone installation assured to be complete practically at least up to the frequency corresponding about 2m in wave
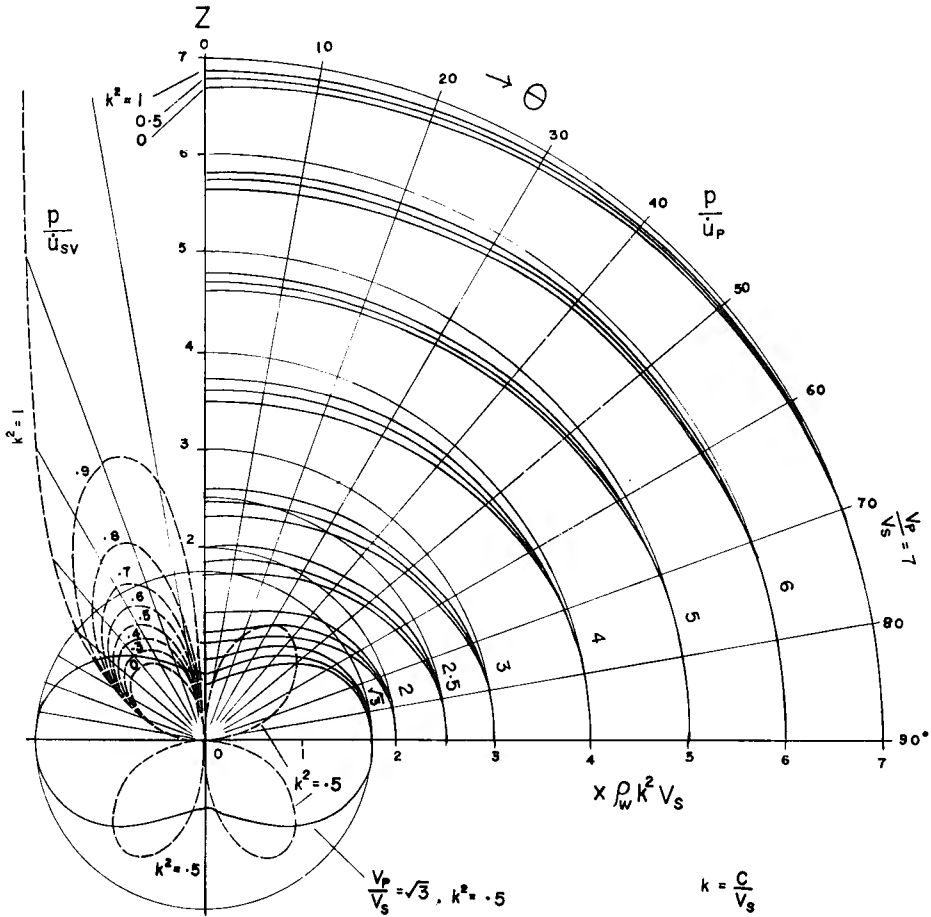
Fig. 3-7. Response of pressure signal to particle velocity of incident waves.
(See Fig. 3-6, Eq. (3-7) and (3-8).)

length of the S wave. Clear record of the S wave detected by a hydrophone is demonstrated in Fig. 3-8 which is cited from the author's previous paper [1967 a].

In this experiment, approximate order of $p/\dot{u}_{SV}$ coincided with the value calculated from Eq. 3-8. However, complete directional pattern of $p/\dot{u}_{SV}$ satisfying Eq. 3-8 was not obtained due to complexity of media.

  (4) Usually in soils value of $p/\dot{u}_P$ is somewhat larger than the value expected from Eq. (3-7), where measured value of V_B is applied. This is considered to be due to loosening of soil near hole wall (Kitsunezaki [1967 a]). In Eq. (3-7) and (3-8), media surrounding a hole is assumed to be homogeneous and isotropic. In real soils, rigidity of media near the hole wall, however, is considered to be lowered as discussed in Section 8-1. By assuming such a simplified model of media as shown in Fig. 3-9 (b), it is conducted after some calculations that the pressure signal (p') of this case
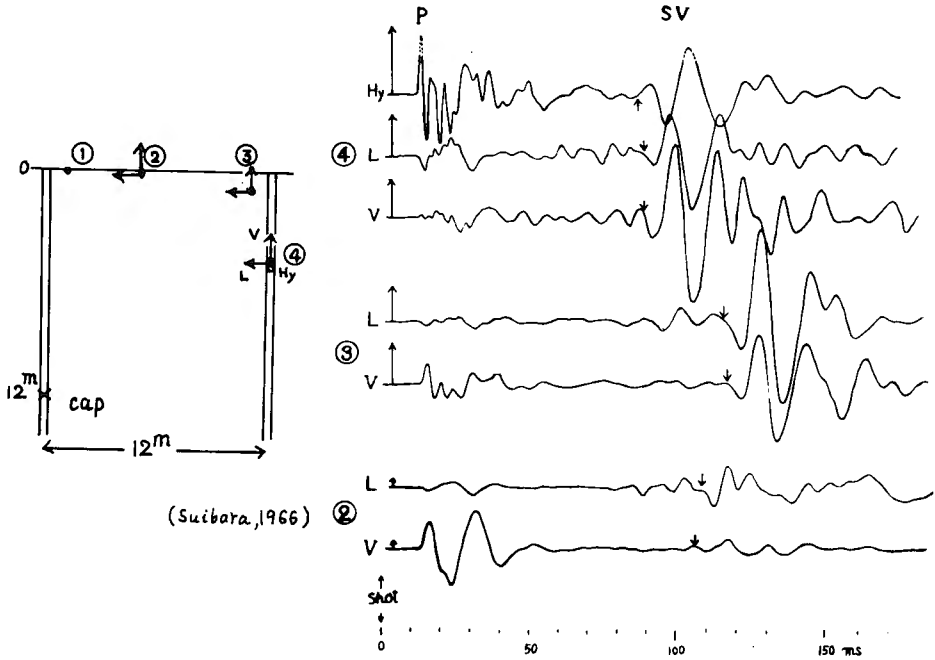
122   C. KITSUNEZAKI

Fig. 3–8. SV wave detected by a hydrophone. **Hy** : hydrophone

has the following relation as to the one (p) in the ideal case given by Eq. (3–7).

$$\frac{p'}{p} = \frac{p'/\dot{u}_P}{p/\dot{u}_P} \div \frac{\mu}{\mu'} \div \left(\frac{V_B}{V_B'}\right)^2 = \left(\frac{V_B}{V_S}\right)^2\left(\frac{V_S}{V_B'}\right)^2 = \frac{\rho}{\rho_w}\frac{1}{k^2} \quad (3\text{–}9)$$

where the conditions, $(V_P/V_S)^2 \gg 1$ and $V_S/V_w \ll 1$ are assumed. (They are satisfied in usual water-saturated soils.) Particle velocity measured on hole wall is the same in both cases and coincides with that of incident wave, as far as wavelength of the incident wave is sufficiently larger than the hole diameter and scale of the loosened region. Meaning of μ' will be explained in Section 8. V_B' is V_B in the model of Fig. 3-9(b). In such a soil as $(V_P/V_S)^2 = r^2 \gg 1$, Eq. (3–7) is simplified as follows;

$$\frac{p}{\dot{u}_P} \doteqdot k^2 \rho_w V_P \ . \quad (3\text{–}10)$$

Hence

$$\frac{p'}{\dot{u}_P} = \frac{p'}{p}\frac{p}{\dot{u}_P} \doteqdot \rho V_P \ . \quad (3\text{–}11)$$

The observed result on $p/\dot{u}_P$ in real soils (sand, clay, silt; $r > 5$) is shown in Fig. 3-9 (a). From this

$$k^2 \rho_w V_P < (p/\dot{u}_P)_{obs.} < \rho V_P.$$
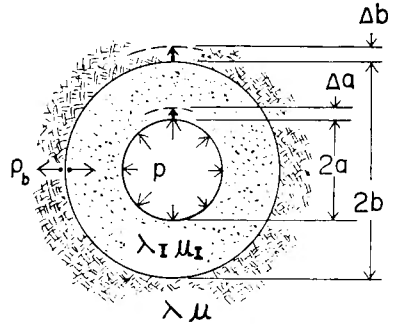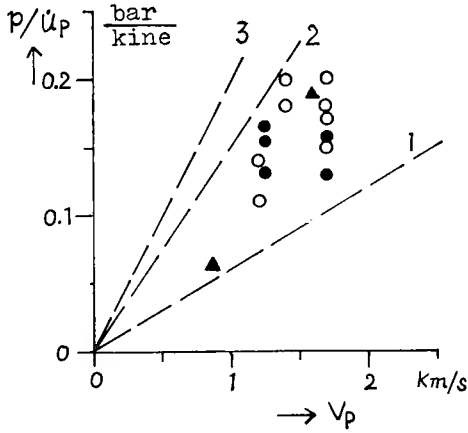
Fig. 3–9(a). Observed value of $p/\dot{u}_P$.

1 $p/\dot{u}_P = k^2\, \rho_w\, V_P$, $(k^2\, \rho_w \equiv 0.6\ g/cm^3)$.

2 $p/\dot{u}_P = \rho\, V_P$, $(\rho = 1.5\ g/cm^3)$.

3 $p/\dot{u}_P = \rho\, V_P$, $(\rho \equiv 2\ g/cm^3)$.

Fig. 3–9(b). A model showing rigidity lowering near the hole wall.

(5) When a hydrophone is set at the bottom of a hole, pressure signal generated by piston-like motion of the bottom is superposed on the one induced by the cause mentioned in (3). The latter is deduced by slight modification of Eq. (3–7) and

Fig. 3–10. An example of records showing S wave detected by hydrophones set in bottom of drill holes (1.5m in depth). Rock : black shist

Eq. (3–8) as to contribution range of z axis and reflection at the bottom (complete reflection is assumed). Result of the calculation becomes as follows.

$$\frac{p}{\dot{u}_P} = \rho_w V_B \left(\frac{k\gamma(1-2\gamma^{-2}\cos^2\theta)}{1+k\gamma^{-1}\cos\theta} + \cos\theta \right) \tag{3-12}$$

$$\frac{p}{\dot{u}_{SV}} = \rho_w V_B \left(\frac{k\sin 2\theta}{1+k\cos\theta} - \sin\theta \right) \tag{3-13}$$

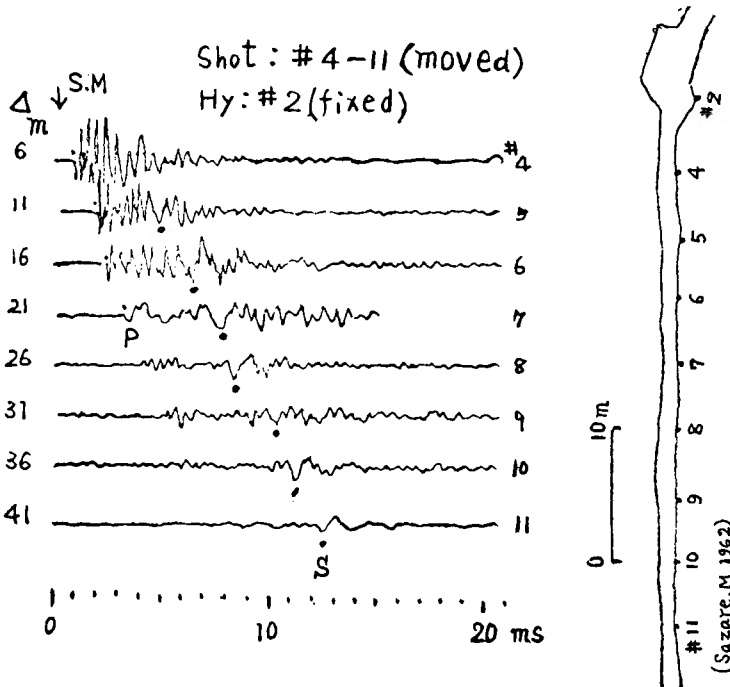In this case the hydrophone reacts also to the SV wave incident normally to the hole axis. Based on this idea, the S wave was detected by hydrophones put in bottom of drill holes in a drift. This example is shown in Fig. 3–10.

(6) Wave detection by a hydrophone in a hole is easy in practice. The wave train, however, sometimes severely disturbed by water waves (tube wave) propagating in a hole independently. For example, a fractured zone in rock behaves as an effective source of tube wave when a P wave is incident to it. Water contained in fractured zone is squeezed out and pushed into the hole by pressure of the P wave. An example of record as to this phenomenon is shown in Fig. 3–11.
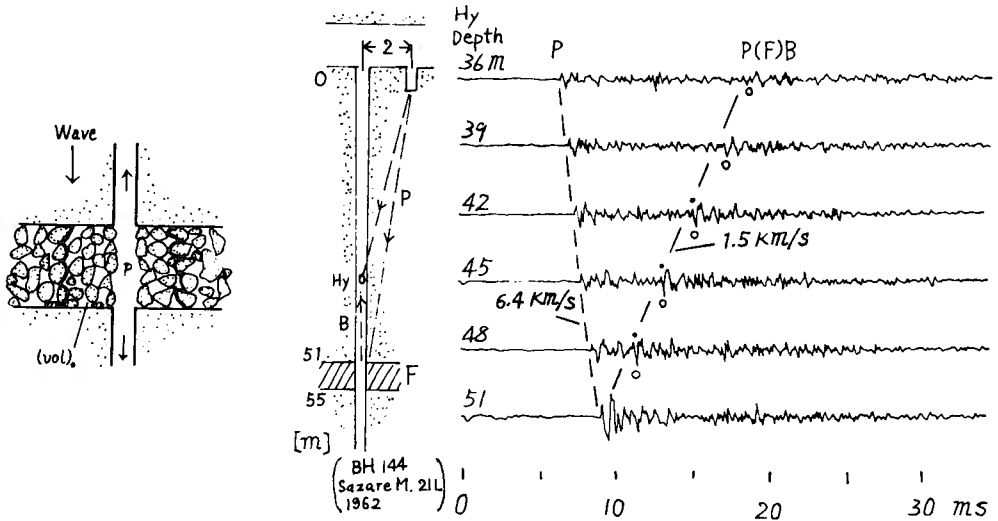
Fig. 3–11. Tube wave generated at a fractured zone by incidence of P wave.
  Rock : black shist

    In short drill holes, resonance of tube wave sometimes severely disturbs normal recording of seismic waves.

    (7) Hydrophones used at the present experiments are composed of cylindrical tube of an electrostrictive ceramic and a matching transformer. Due to its electro-mechanical characteristics, they have very flat transfer characteristics in higher frequency range, which can be easily calibrated by application of an electrical circuit

technique (Kitsunezaki [1967 a]). Absolute sensitivity of a hydrophone was calibrated by vibrating it within water contained in a vessel set on a vibration table. In relatively lower frequency, pressure signal, p, delivered to the hydrophone is expressed by the following relation;

$$p = \rho_w \, H \, \ddot{u},$$

where

ρ_w = density of water,

H = water depth of the hydrophone measured from free surface of water,

$\ddot{u}$ = accelaration of vibration.

4. Generation of Shear Wave

4–1 Seismic waves generated by point force systems

For convenience to the succeeding discussions formulae as to waves generated by a point force systems in infinite media will be shown in the following, based on White's expression [1965].

(1) Single point force

We assume that body force F acts an infinitesimal volume of media at the origin of the coordinate in the direction along z axis.

$$F = k \, G \, g(t) \qquad (4\text{–}1)$$

where k is unit vector of z direction. Assuming the spherical coordinate (r, θ, ψ), the displacement (u) radiated from the point force is expressed as follows,

$$u_{P,r} = \frac{G \cos \theta}{4\pi \, \rho r} \left[\frac{1}{V_P{}^2} g \left(t - \frac{r}{V_P} \right) + \frac{2}{r V_P} g^{\mathrm{I}} \left(t - \frac{r}{V_P} \right) \right.$$
$$\left. + \frac{2}{r^2} g^{\mathrm{II}} \left(t - \frac{r}{V_P} \right) \right]$$

$$u_{P,\theta} = \frac{G \sin \theta}{4\pi \, \rho r} \left[\frac{1}{r V_P} g^{\mathrm{I}} \left(t - \frac{r}{V_P} \right) + \frac{1}{r^2} g^{\mathrm{II}} \left(t - \frac{r}{V_P} \right) \right] \tag{4–2}$$

$$u_{S,r} = -\frac{G \cos \theta}{4\pi \, \rho r} \left[\frac{2}{r V_S} g^{\mathrm{I}} \left(t - \frac{r}{V_S} \right) + \frac{2}{r^2} g^{\mathrm{II}} \left(t - \frac{r}{V_S} \right) \right]$$

$$u_{S,\theta} = -\frac{G \sin \theta}{4\pi \, \rho r} \left[\frac{1}{V_S{}^2} g \left(t - \frac{r}{V_S} \right) + \frac{1}{r V_S} g^{\mathrm{I}} \left(t - \frac{r}{V_S} \right) \right. \tag{4–3}$$
$$\left. + \frac{1}{r^2} g^{\mathrm{II}} \left(t - \frac{r}{V_S} \right) \right]$$

$$u_{P,\psi} = 0$$

$$u_{S,\psi} = 0 \, ,$$

where

$$g^{\mathrm{I}}(t) = \int_{-\infty}^{t} g(t')\,dt'$$

$$g^{\mathrm{II}}(t) = \int_{-\infty}^{t} g^{\mathrm{I}}(t')\,dt' . \qquad\qquad (4\text{--}4)$$

Suffixes, "P" and "S", indicate symbols as to P and S wave.

Suffixes, "r" and "θ", incdicate symbols of r and θ components.

If the radial distance from the source is sufficently larger than the wave length,

$$u_{P,r} = \frac{G\cos\theta}{4\pi\,\rho\,V_P{}^2\,r}\; g\left(t - \frac{r}{V_P}\right)$$

$$u_{S,\theta} = -\frac{G\sin\theta}{4\pi\,\rho\,V_S{}^2\,r}\; g\left(t - \frac{r}{V_S}\right). \qquad\qquad (4\text{--}5)$$

Terms as to g^{I} and g^{II} in Eq. (4–2) and (4–3) are so called near field terms, which are effective only at short distances. Some simple sources can be made by combinations of single point force mentioned above. The cases in relation with further discussions will be shown in the following.

(2) *Double force without moment*

This is a case that two forces, F and $-F$, act on two points of $(h, 0, 0)$ and $(-h, 0, 0)$ respectively, where h is very small distance. Expressions for the radiated displacements are as follows,

$$u_{P,r} = \frac{2h\,G\cos^2\theta}{4\pi\,\rho\,V_P{}^3\,r}\;\dot{g}\left(t - \frac{r}{V_P}\right)$$

$$u_{S,\theta} = -\frac{hG\sin 2\theta}{4\pi\,\rho\,V_S{}^3\,r}\;\dot{g}\left(t - \frac{r}{V_S}\right). \qquad\qquad (4\text{--}6)$$

(3) *Equi- expansive source*

We think about a very small spherical cavity of radius a, subjected by pressure $p = Pg(t)$. Expression for the radiated displacement is

$$u_{P,r} = \frac{P\,a^3}{4\,V_S{}^2\,V_P\,\rho r}\;\dot{g}\left(t - \frac{r}{V_P}\right). \qquad\qquad (4\text{--}7)$$

Of course, the shear wave is not radiated. Eq. (4–7) can be applicable in larger distances.

4–2 Shear wave generated by a small explosion

In a small explosion, the most important factor controlling radiation pattern of source is hole itself. Two types of explosion source will be discussed in the following.

(1) *Explosion at the bottom of short hole*

In this case, tamped material (usually water or clay) is pushed out simultaneously

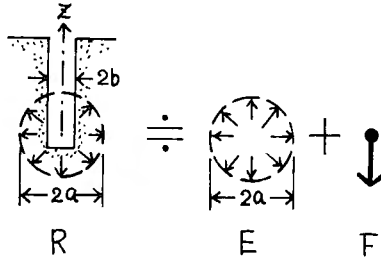with explosion. Fundamental characters of the source can be simplified as a model (R) shown in Fig. 4–1.

Fig. 4–1. Source model corresponding to small explosion at the bottom of a short hole.

This is an expansive source in which effective pressure lacks on the side of open hole. In Fig. 4–1, this is considered as combination of a complete equi-expansion source (E) and a single point force (F). Expressions for radiated displacement corresponding to F and E can be found in Eq. (4–5) and (4–7) respectively. We assume that radius of effective spherical cavity is a and hole radius is b. Hole section may be regarded as pressure-lacked area on the cavity surface approximately. Therefore, P in Eq. (4–7) can be connected to G in Eq. (4–5);

$$G = - \pi b^2 P .\qquad (4\text{–}8)$$

In the following expression, symbol as to a single point force, a double force and an expansion source will be expressed by being attached suffixes of F, D and E respectively.

In the present source,

$$u_{P,r} = (u_P)_F + (u_P)_E$$

$$= \frac{b^2 P}{4 V_P^2 \rho r} \left\{ \frac{a^3}{b^2} \frac{V_P}{V_S^2} \dot{g}\left(t - \frac{r}{V_P}\right) - \cos \theta \cdot g\left(t - \frac{r}{V_P}\right)\right\} \qquad (4\text{–}9)$$

$$u_{S,\theta} = (u_{S,\theta})_F = \frac{b^2 P \sin \theta}{4 V_S^2 \rho r} \, g\left(t - \frac{r}{V_S}\right). \qquad (4\text{–}10)$$

If

$$g(t) = e^{j\omega t},$$

$$u_P = \frac{b^2 P}{4 V_P^2 \rho r} \left\{ j\left(\frac{a}{b}\right)^2 \left(\frac{V_P}{V_S}\right)\left(\frac{\omega a}{V_S}\right) - \cos \theta\right\} e^{j\omega\,(t - r/V_P)} \qquad (4\text{–}11)$$

If $\omega a / V_S \ll 1$, characteristics of the single force dominate. The above expressions are valid only in such a condition as $\omega a / V_S \ll 1$. Therefore, we can not say too

much about the characteristics of shorter wave length, where predominant components of particle velocity may exist under the usual shot condition.

The author has already demonstrated many examples of the S wave records corresponding to this kind of shot in the previous papers [1960a, 1960b, 1961, 1964, 1965].

Shot A 1   (Myōhō M., 1960)
↓ (22 g) (Tamp : clay)
(0m.)

A4
(15m.)

A5
(20m)

A6
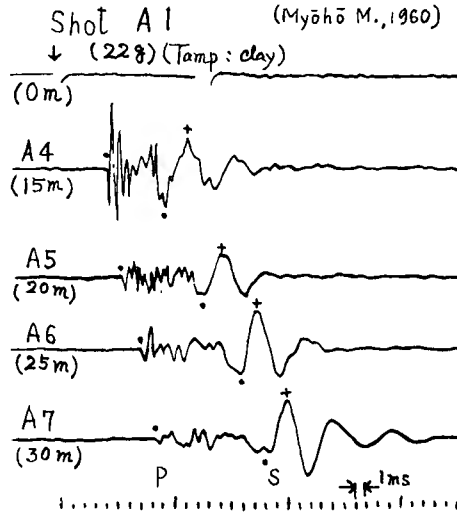(25m)

A7
(30m)   P   S   →|←¹ms

Fig. 4–2. Example of records showing P and S
waves generated by a small explosion in drift.
spread : along drift (about 2m in diameter).
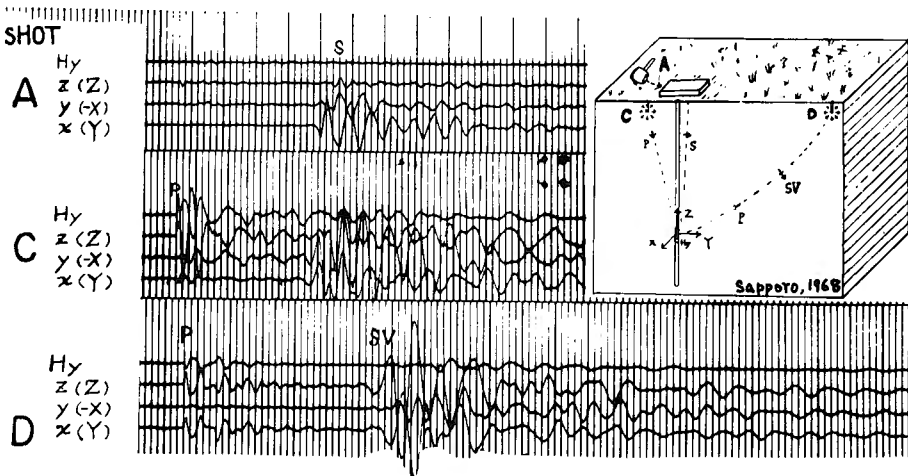V_P=3.4 km/s, V_S=1.7 km/s, sandstone

Fig. 4–3. Examples of the record obtained in borehole. Comparison of the waves from the
different kinds of source, A, C and D. Depth of the borehole geophone is 51m.

Only a few typical records showing the S wave are cited from the previous papers. Fig. 4–2 shows a record obtained in mine drift (tertiary sand-stone). All depth of the shot and geophones were 1.5m. Geophones are fixed with cement at hole bottoms (Kitsunezaki [1960b]).

D of Fig. 4–3 (cited from Kitsunezaki and Goto [1969]) shows P and S waves generated by a small shot in a hole (about 1m in depth) near the ground surface. The media near the shot point was sand. Dynamite was tamped by water. The record was obtained by the borehole geophone of Fig. 3–4 (b).

Though the records, which allow complete discussion of source mechanism, have not obtained, it was ascertained by the author [1965]* that space distribution of sense of particle motion coincides with the one expected from Eq. (4–10). As discussed in Section 2, propagation of the S wave is essentially free from existence of boundary surface. Such a proof can be found in Fig. 12 of the suthor's previous paper [1965].

(2) *Explosion in intermediate depth of long hole*

1) Source model of this case is shown in Fig. 4–4. Essence of idea is the same as the preceeding case and it has been already discussed in the author's previous paper [1967].
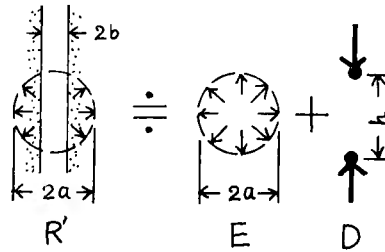
Fig. 4–4. Source model corresponding to small explosion in a long hole.

$$u_P = (u_P)_E + (u_P)_D$$

$$u_S = (u_s)_D$$

$$G = -\pi b^2 P .$$

Therefore,

$$u_{P,r} = -\frac{P a^3}{4 V_S{}^2 V_P \rho r} \left\{1 - 2\left(\frac{b}{a}\right)^2 \left(\frac{V_S}{V_P}\right)^2 \cos {}^2\theta\right\} \dot{g}\left(t - \frac{r}{V_P}\right)$$

$$u_{S,\theta} = \frac{P ab^2 \sin 2\theta}{4 V_S{}^3 \rho r} \cdot \dot{g}\left(t - \frac{r}{V_S}\right)$$

(4–12)

From assumption,

---

* Fig. 14 of the author's previous paper [1965] involves an error. Position of L and T written in left side of the figure should be replaced mutually.

$$b/a \leqq 1.$$

Some characteristics of this source will be shown in the follownig.

$$
\left.
\begin{aligned}
\frac{(u_P)_{min}}{(u_P)_{max}} &= \frac{(u_P)_{\theta=0,\pi}}{(u_P)_{\theta=\pi/2}} = 1 - 2\left(\frac{b}{a}\right)^2\left(\frac{V_S}{V_P}\right)^2 \\
\frac{(u_S)_{max}}{(u_P)_{max}} &= \frac{(u_S)_{\theta=\pi/4,3\pi/4}}{(u_P)_{\theta=\pi/2}} = \left(\frac{b}{a}\right)^2\left(\frac{V_P}{V_S}\right)
\end{aligned}
\right\}
\qquad (4\text{-}13)
$$

Amplitude ratio of the radiated S wave displacement (or velocity) to the P wave one is affected by (b/a) and (V_P/V_S), and it becomes larger at larger b/a. Experimental results in soil suggested approximate conformity of the above model as to radiation pattern, though complete experimental check has not been carried out (Kitsunezaki [1967 (b)]). Fig. 3–8 is also an example of such a source. Fig. 4–5 is an example of records obtained by a small shot (cap alone) in a hole. The experimental work mentioned above were carried out in mine drift (paleozic phyllite) (Kitsunezaki [1961]).
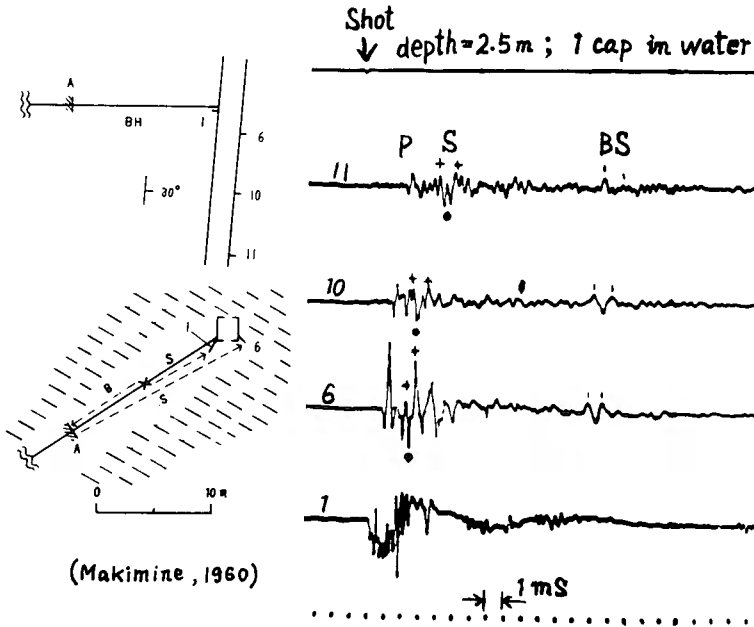

Fig. 4–5. Example of record obtained by a small explosion in a hole.
   Situation : mine drift
   Rock   : phyllite
   PU   : fixed in bottom of holes.
   A   : a position of hole closed by crush.

2) Yoshimura and others [1971] analyzed the experimental results as to a small explosion in a borehole. Connecting their data with White and Sengbush's

[1963], they tentatively concluded that the angle of maximum radiation of the S wave depends of V_P/V_S. For larger V_P/V_S, the corresponding θ becomes larger. (According to them, $\theta \fallingdotseq 45°$ for $V_P/V_S = 6.2$, $\theta \fallingdotseq 65°$ for $V_P/V_S = 9.5$) And then, radiation pattern of their experiment has sharper peak than the one expected from Eq. (4–12).

The author thinks that delicate discussion is somewhat too early, considering incompletness* of the experimental procedures, complexity of the real soil and insufficient numbers of the data. It is more necessary to draw a rough sketch catching essence of phenomena. From the above point of view, their results are considered to be rather conformable with the author's model as the first approximation.

More exact and much data should be gathered in variable conditions, comparing with the simple model. The discrepancy will be very natural, especially in soils because of their complexity. In the next step, the discrepancy will be discussed. One of important factors affecting radiation pattern may be the rupture of media with crack which may be strongly affected by inhomogeneous and anisotropic characters of earth materials (Kisslinger et al. [1961]).

3) Refering to White and others' experiment [1963], their case is such a particular one as tube wave velocity in a hole is slightly higher than the S wave velocity of surrounding media, where the tube wave can not exist as a surface wave. In this condition, the energy of the tube (water) wave is radiated from the water to the solid. This modifies radiation pattern of the S wave strongly. Usually, the tube wave velocity is slower than the S wave velocity of solid. Hence, the body waves can not be radiated from the tube wave. In this meaning, tube wave belongs to the surface wave.

(3) *Predominant wavelength*

1) Predominant frequency of body waves radiated from an explosion source of certain amount of charge is strongly affected by properties of media. Of course, it is higher in harder rock and lower in softer soil. For example, as to explosion of one cap it distributes in *50–3000cps*. Nevertheless, wavelength of radiated waves is rather constant, roughly speaking. This property is shown in Fig. 4–6.

2) As well known, the predominant frequency becomes lower with increase of propagation distance due to attenuation effects. Another cause to disturb the normal detection of the predominant frequency is cut-off characteristics of recording system. The data in Fig. 4–6 are picked up from many data obtained for the other purposes by the author.** Data, in which predominant frequency may be effectively modified by attenuation and instrumental characteristics, have been rejected from those in Fig. 4–6. The safety range of distance, where the wave pulse is approximately free from the attenuation effects, is decided individually, observing change of pulse width. General consideration as to this safety range will be discussed in Section 6.

---

* In their experiment, consideration was not sufficient to compensate attenuation effect on wave amplitude.
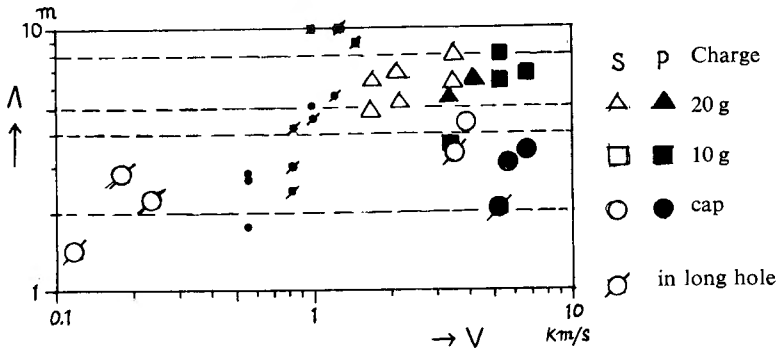** One datum obtained by Oyo-chishitsu Co. is also included in Fig. 4–6.

Fig. 4–6. Relation between velocity of P and S wave and their predominant
    wavelength near source.
    $V = V_P$ or V_S, $\Lambda = \Lambda_P$ or Λ_S
    small marks : Λ_P in soils.

Predominant period of the wave pulse T is directly read from peak-peak interval
of wave trains on records, and then converted to wavelength (Λ) by such a formula
as $\Lambda_S = V_S T_S$ (or $\Lambda_P = V_P T_P$), where V_S (or V_P) is propagation velocity near the
source.

3) From Fig. 4–6, it is known that the predominant wavelength is 2–4m as
to one cap (about 3×10^3 joule in thermal energy) and 5–8m as to dynamite of 20g
(about 100×10^3 joule), If values of Λ_P in soil ($V_P/V_S > 4$) are rejected. Such Λ_P
values are also plotted only for reference. They seem to have problems on reliability
of data and analytical expression.

4–3   SH type source

The SH wave is more convenient in analysis than the SV wave. It is not easy
to generate the SH wave in near ground surface by an explosion. In near ground
surface, vertical holes are easier to be drilled. Hence, by the above reason and ex-
istance of surface condition, the S wave generated by an explosion becomes usually
a SV wave. Sometimes, the SH waves can be generated also by usual explosion and
vertical shock with a hammer. Its generation, however, is unstable as to magnitude
and radiation pattern, because inhomogeneity of medium properties may be a key
factor governing it.

As the stable SH wave source, certain mechanical shocks are usually employed.
It is common in any methods to make horizontal force act on the ground. As refered
in introduction already, a wooden plate (about $3 \times 0.4 \times 0.1$m) pressed on the ground
with proper load is widely used for this purpose. This plate is struck horizontally
with a hammer by human power to generate the SH wave. The author also has
applied this method as the source for refraction prospecting by the SH wave and
as the source on the ground surface for S wave logging in a borehole. The longest
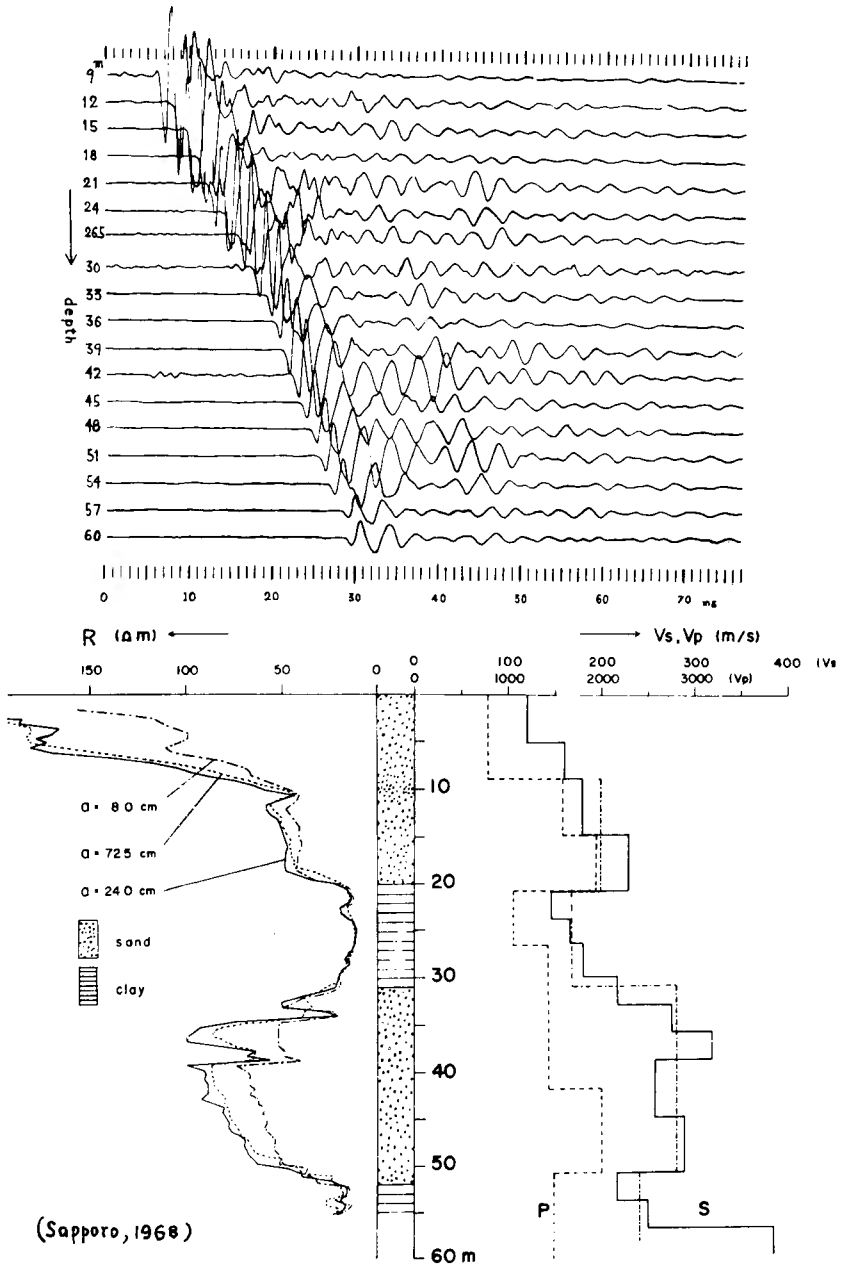limit of propagation distance from this source is about 100m from practical point

Fig. 4–7. Record for S wave logging obtained by horizontal hammering on the ground surface as source, and logging data at the same place.

of view.

In Fig. 4–3, this method (A) is illustrated with a record obtained. The author does not want to say too much as to this method, because this is very well known. Only an example is shown in Fig. 4–7. Fig. 4–7 is full record over the whole borehole length, composed from individual traces of the S waves as shown in Fig. 4–3.

4–4   Mechanical source applied in a borehole

(*1*) As discussed in Section 7, it is necessary for complete logging that a source is also inserted in a borehole with detectors. S wave logging can be completed by developing such a practical source. The author is in the course of research as to this. Idea of author's approach and some experimental results will be introduced in the following.

(*2*) The author's idea is based on the experiments in mine drifts. Decreasing the whole scale including wavelengths and diameters of drifts, we can get a model of borehole problems. The author has already refered to S wave generation by small shots or hammering in mine drifts. As far as the S wave generation is concerned, the explosion effect is also the same as hammering, because the essential dynamic action of it is that of a single point force.

(*3*) In general, if a source exists in infinite homogeneous media, displacements of body waves radiated can be expressed as summation of effects of the following factors as shown by Case and Colwell [1967] (Nakano and Okano [1970]).

$$F_i = \int_S f_i \, dS$$

$$L_{ij} = \int_S r_i' f_j \, dS$$

$$T_{ij} = (1/2) \int_S (n_i u_j + n_j u_i) \, dS$$

where f means force (per unit area) acting on the source surface, r' is position vector at any point of the source surface, n is unit vector of the source surface, u is displacement at the source surface. Suffix "i" etc. indicate component of vectors. Integral is done as to the whole surface of the source "S". The whole of terms involving F_i will be expressed by $[F_i]$, for example.

$$u_S(or\ u_P) = [F_i] + [L_{ij}] + [T_{ij}]$$

All terms involved in $[L_{ij}]$ and $[T_{ij}]$ have a factor of a/Λ, where a means a typical dimension of the source and Λ is wavelength of the radiated waves. But the corresponding factors in $[F_i]$ do not depend on Λ. Hence, if the wavelength of the radiated waves is sufficiently larger than a typical dimension of the source, $[F_i]$ usually dominates over $[L_{ij}]+[T_{ij}]$, as far as F_i is not identically zero;

$$u_S(or\ u_P) \doteqdot [F_i] \quad \text{for} \quad a/\Lambda \ll 1 \text{ and } F_i \neq 0.$$

This fact was noted by Case and Colwell. F_i is so-called total force over the source surface. L_{ij} and T_{ij} have a character of doublet or moment. Single point force, of course, corresponds to F_i.

(4) In order to practise S wave logging normally, the following relation should be held,

$$\text{wavelength} \gg \text{hole diameter}.$$

In such wavelength, distortion of the waves due to the hole boundary and the near surface effects is negligible and also free from the disturbance of surface waves. This assures exact detection of the S wave. P wave velocity is the highest in general and such consideration is not necessary for velocity logging of P wave. Since size of source in radial direction is limited by hole diameter;

$$\text{size of source} < \text{hole diameter}.$$

A long source along hole axis is not favourable*, when the waves propagating along hole axis is to be detected.

Therefore the scale of the source may be sufficiently less than the wavelength, and the application of $[F_i]$ is easier because of its predominant character mentioned in (3). Such $[T_i]$ as a torsional force serves as purer source of the S wave. However even small F_i born by unbalance of source mechanism may prevent satisfactory results.

When the S wave is radiated in radial direction, design of such a torsional source becomes easier than the case of axial radiation mentioned above. One of the reasons is that longer dimension of source can be applicable.

(5) By the reason mentioned above, as the first step of the experiment, the author designed the mechanical source which makes single force act to the hole wall. The mechanism was what is called the solenoid hammer by the author [1970c]. This is electro-magnet of plunger type which is especially designed to make the plunger serve as a hammer.

The schematic view of this is shown in Fig. 4–8 with the circuit.
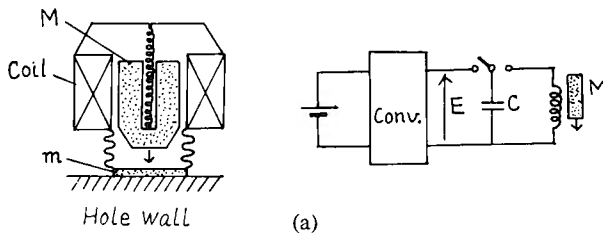
Fig. 4–8(a). Schematic view of S wave source and the circuit.

* This means that initial kick of the wave becomes ambiguous. However, this problem itself may be overcome by using such a technique as compare the whole wave form of adjoining points.
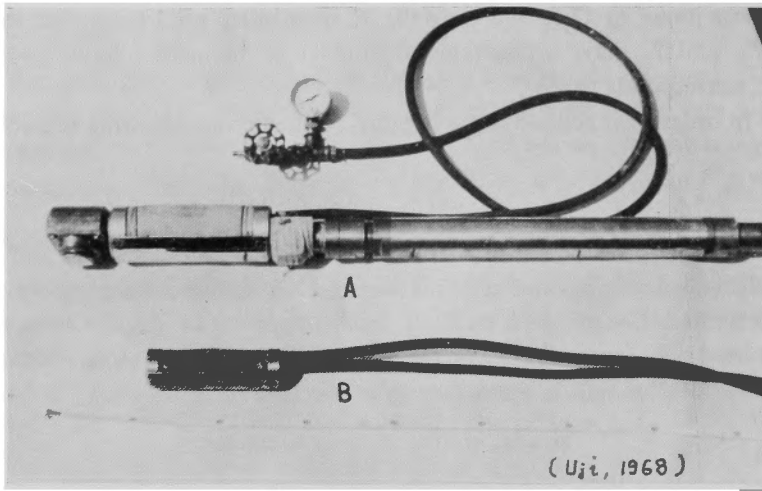
(b)

Fig. 4–8(b).   Photographic view
A S source   **B** : geophone

The hammer (plunger) is operated by discharging a condenser with large capacity to the solenoid. The condenser is charged through DC→DC convertor by a battery. Voltage of the condenser at fully charge is about 300–500volt (about 2×10 joule in electrical energy).

Combination of a hammer mass (M) and an effective elastic stiffness ($K_\perp$) of media near the source area serves as a resonance system, which is effective while both are contacted. The resonance frequency and the stiffness are given by Eq. (3–1) and Eq. (3–2). The hammer and the media surface keep contact for a half period
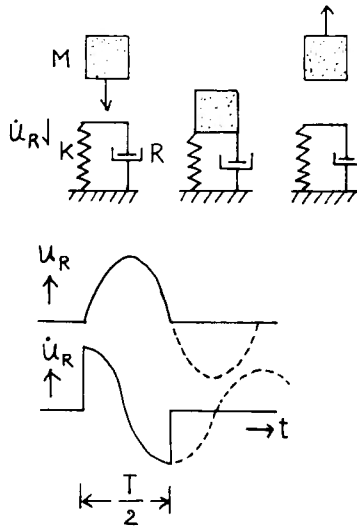
Fig. 4–9. Illustration of impulsion process.

from the first instant of impulsion. And then, the hammer is repulsed from the media surface. This process is illustrated in Fig. 4–9.

In Fig. 4–9 u_R means displacement of the source plane, to which the force acts. Both are in proportion. Hence the wave form of displacement radiated becomes the same as u_R. Usually we observe particle velocity. From Fig. 4–9, we can assume that one period of particle velocity of the radiated wave corresponds to a half period of the resonance system approximately. Hence, from Eq. (3–6)

$$\lambda_R \doteqdot \frac{\lambda_{0\perp}}{2} \doteqdot \frac{\pi}{2}\sqrt{\frac{M}{\rho b}} \qquad (4\text{--}14)$$

where λ_R is predominant wavelength (S wave) of particle velocity radiated.

The wavelength of the S wave radiated from such an impulsion type source does not depend on properties of media. The characteristic that wavelength is constant is very favourable for S wave logging. And then, efficiency (η_R) of energy conversion from the hammer to seismic waves is also constant, in spite of variety of media properties. Those are the merits of the source of hammer type.

Liquid-like friction (R) in Fig. 4–9, is obtained by estimating energy radiated as seismic waves, if inelastic properties of media is neglected. Assuming that the wavelength is sufficiently larger than the hole diameter and the hole diameter is also sufficiently larger than size of the source area as well as in the case of Eq. (4–14), R becomes as follows (Kitsunezaki [1970]),

$$R = \frac{8c^2}{3\pi}(1-r^{-2})^2\left(1+\frac{1}{2}r^{-3}\right)\rho b^2\, V_S$$
$$\doteqdot 0.73\,(1-r^{-2})^2\,\rho b^2\, V_S \qquad (4\text{--}15)$$

Damping constant (h) of this system is expressed as

$$h \equiv \frac{R}{2M\omega_0}$$
$$= \frac{2}{3\pi}\,c^{3/2}(1-r^{-2})^{3/2}\left(1+\frac{r^{-3}}{2}\right)\left(\frac{\rho b^3}{M}\right)^{1/2}$$
$$\doteqdot 0.19\left(1-\frac{3}{2}r^{-2}\right)\left(\frac{\rho b^3}{M}\right)^{1/2}. \qquad (4\text{--}16)$$

$$h \doteqdot 0.2\left(\frac{\rho b^3}{M}\right)^{1/2} \quad : \quad r^2 \gg 1$$

$$\eta_R = 1 - e^{-2\pi h/\sqrt{1-h^2}} \qquad (4\text{--}17)$$

$$\eta_R \doteqdot 2\pi h \quad : \quad 2\pi h/\sqrt{1-h^2} \ll 1 \qquad (4\text{--}18)$$

In an actual system, a rigid plate (radiation plate) is inserted between the hammer and the media. By effect of this mass (m), the preceeding formulae are modified

as follow;

$$.1_R \doteqdot \frac{\pi}{2} \sqrt{\frac{M+m}{\rho b}} \tag{4-19}$$

$$\eta_R \doteqdot \frac{1}{1+m/M} (1 - e^{-2\pi h/\sqrt{1-h^2}}) \tag{4-20}$$
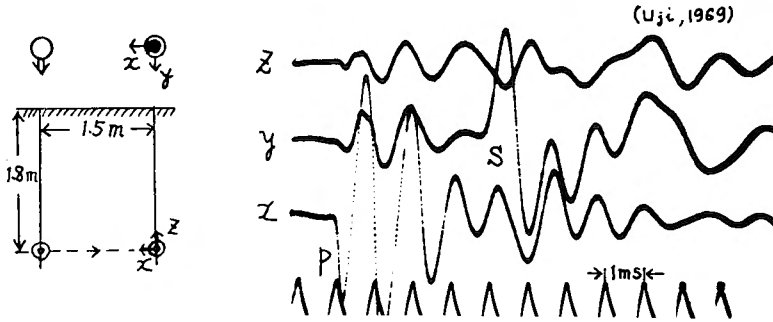

Fig. 4-10. Examples of records obtained with mechanical source for S wave.
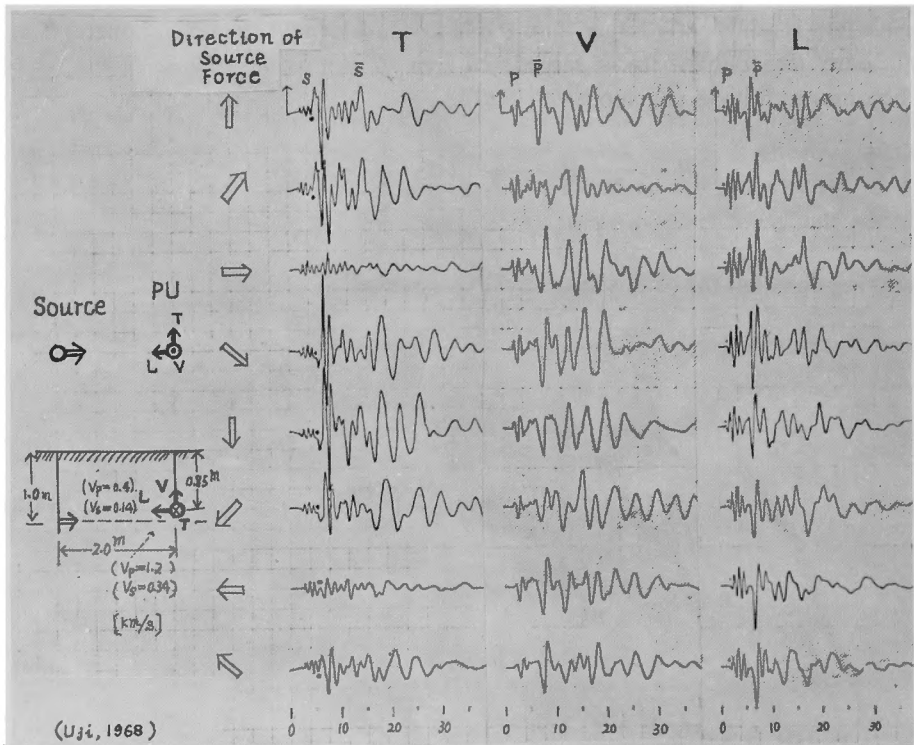
Fig. 4-11. Record obtained with mechanical source for S. They show how radiated amplitude depends on direction of the source force.
  PU : fixed.   Source : rotated and fixed in each direction.

Deduction of η_R is based on empirical relations obtained by one-dimensional wave experiment by the author.

(6) Examples of records are shown in Fig. 4–10, where the waves are propagating horizontally. The records in Fig. 4–11 show radiation pattern of the waves. Experimental site consists of horizontal multi-layer. So, wave trace becomes somewhat complicated. As far as transverse component (T) is concerned, radiated amplitude regularly depends on direction of the source force, which is also shown in Fig. 4–12.
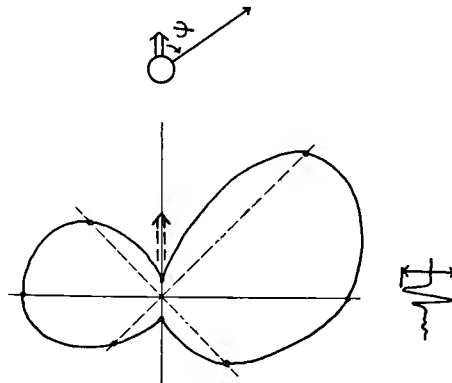
Fig. 4–12. Radiation pattern of T component ("S" phase) obtained from Fig. 4–11.

In Fig. 4–11 $\bar{S}$ and $\bar{P}$ are direct waves. S and P are refracted waves from deeper layer of higher velocity. In this figure, a geophone body is fixed through the whole experiment, and the source (force direction) is rotated. Medium were clay both in Fig. 4–10 and 4–11.

In Fig. 4–11, the approximate characteristics of the amplitude pattern of transverse component are as those expected from a single point force. For the longitudinal and vertical components, however, those characteristics seem not to depend on direction of the force. As to those characteristics, the source seems to be understood as a combination of a single point force and the equi-expansive source. Existance of equi-expansive source may be due to the fact that some region near the source is in plastic condition over elastic limit (Fig. 4–13).
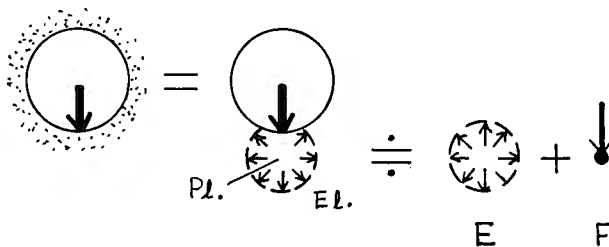
Fig. 4–13. A model explaining physical process of the hammering source in a hole.

The predominant wavelength of the S wave observed was about 0.28m ($=\varLambda_S$), $\varLambda_R$ estimated from Eq. (4–19) was 0.055m.

$$\frac{\varLambda_S}{\varLambda_R} \doteqdot 5$$

Considering the attenuation effect, $\varLambda_S/\varLambda_R$ may become 3–4. Discrepancy of $\varLambda_S$ and $\varLambda_R$ is due to inelastic properties near the source and lowering of elastic constant in near hole surface. For such formulae as Eq. (4–19) and (4–20), too complete conformity should not be expected. Those idealized formulae are to provide practical standard for design purposes, by being modified with empirical correction factors.

5. S wave converted from other kinds of waves

5–1 Conversion from P wave to S wave

(*1*) As generally known, two kinds of seismic body waves (P and S) are usually generated by any one of them incident to a boundary of elastic media. However, in field-experiments of artificial seismic waves, clear detection of such conversion phenomena has not been so common. Complexity of media conditions in the real field makes simple identification of the waves difficult. Therefore, sufficient attentions have not been paid to the problems on the wave conversion mentioned above.

Observation of the waves in boreholes makes the identification of the waves easy and sure. We sometimes observe transmission of predominant S wave converted from the P wave.

(*2*) With increase of field-experiments, it has been known that contrasts of the seismic properties are very large in the medium near the ground surface in general. Therefore, conversion of the waves observed is considered to be very natural. In plain land of Japan, the boundary surfaces converting the waves are usually very shallow in depth (less than about 10m). Such a fact is important in the two sides.

  a) Applying this to practical survey, S wave measurement in wide range of depth in a borehole becomes possible.

  b) Hasty surveys sometimes lead to false analyzed result, by misunderstanding the converted wave as the direct one.

(*3*) The state of the water contained is a common factor which controls seismic properties of soils, especially near the ground surface. The water table usually provides the boundary with clear contrast for P wave velocity. It is not always a considerable boundary for the S wave. As far as S wave velocity does not change (density change neglected), the conversion from P to S can not occur (Kitsunezaki [1967d]). For this reason, the water table is not always an effective boundary for the wave conversion.

However, in general, the water table covered by an impermeable soil layer is also simultaneously the lithological boundary. This provides usually distinct con-

trasts for both P and S wave velocities with for density.

(4)   The incident angle (measured from an axis normal to the boundary) giving maximum conversion, from P to S, is relatively large. It is usually 40°–60°: In order to get larger efficiency of the conversion in the transmitted direction near the normal

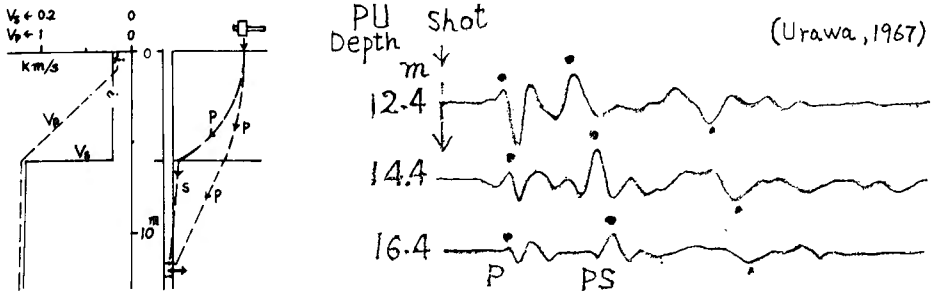Fig. 5–1.   An example of records showing P→S conversion.

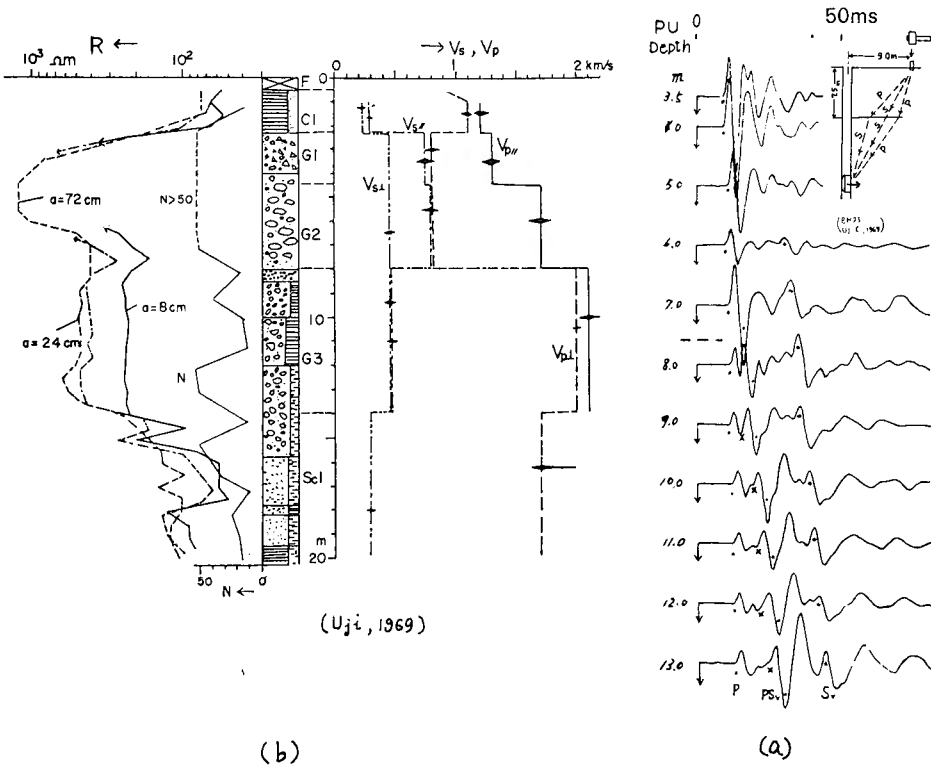(b)   (a)

Fig. 5–2.   Examples of records (a) showing P→S conversion and the corresponding log data (b)

$\quad$ P : P wave, $\qquad$ Sv : direct Sv wave,

PS$_v$: S$_v$ wave converted from P wave,

$\quad$ N : standard penetration value

$\quad$ R : resistivity

axis (usually vertical), it is favourable from geometrical consideration of wave path that the following condition is satisfied.

(a) V_P in an incident side is sufficiently larger than V_S in a transmitted side.

(b)   The boundary interface is near a source.

Both conditions are satisfied in the cases of Fig. 5–1 and Fig. 5–2 explained in the following.

(5)   Examples of records as to the phenomena (P→S conversion) are shown in Fig. 5–1 and Fig. 5–2. The records shown in Fig. 5–1 was obtained at the experiment by the author and staffs of a geological survey company (Oyo-chishitsu Co.) in 1967. The records in Fig. 5–2 were obtained by the author and Goto [1970].

In the field as to Fig. 5–1 and Fig. 5–2, the water tables, which were also boundary of soil materials, served as the boundary for "P→S conversion".

Seismic properties in the site shown in Fig. 5–2 are very peculiar. The gravel layers, G_1 and G_2, have considerable anisotropic properties as discussed in Section 9. The water table is about 8m in depth.

5–2   Conversion, from tube wave to S wave

In hard rock, attenuation of the tube wave is low. Hence strong energy is conveyed by the tube wave to the bottom of borehole. Hammering effect of the tube wave at the bottom serves as a single point force in the solid media. Hence, the P and S waves are radiated from there.

Such a phenomena has not been detected in soils.

An example of the S wave (BS) converted from the tube wave can be observed in Fig. 4–5.

6.   Attenuation of seismic waves

Attenuation constants are also important factors characterizing seismic property of media, as well as propagation velocities. Complete measurement of attenuation characteristics needs certain field conditions. Homogeneous media is favourable. Complex structures disturb regularity of amplitude decay of the wave. Though corrections for them are possible in relatively simple case (Kitsunezaki [1967b]), large amount of correction always makes accuracy of analysis low.

Frequency dependency of attenuation constants is one of focuses in research of seismic waves. The author has not the necessary original data to allow comprehensive discussion about this problem. Recently, attenuation constants have been considered to be in proportion of one power to frequency, at least in rocks and granular soils (Mcdonald et al. [1951], White [1965]). In this paper, the author will discuss some restricted problems as to attenuation.

(1)   *Relation between attenuation of pulse-form waves and that of sinusoidal waves*

1)   As the first step of discussion, fundamental relations conformable to the

frequency dependency mentioned above are introduced here, based on White [1965].

Usual relations between stress and strain in an ideal elastic media are applicable also here, by putting $\lambda + j(\omega/|\omega|)\lambda'$ and $\mu + j(\omega/|\omega|)\mu'$ instead of λ and μ respectively.

The expression for a sinusoidal plane wave in the positive direction is

$$u = u_0\, e^{-(|\omega|\theta/2V)x}\, e^{j\omega(t-x/V)}\,,\tag{6-1}$$

where

$$V = \begin{cases} \sqrt{(\lambda+2\mu)/\rho} & (= V_P) \\ \sqrt{\mu/\rho} & (= V_S) \end{cases}$$

$$\theta = \begin{cases} (\lambda'+2\mu')/(\lambda+2\mu) & (= \theta_P) \\ \mu'/\mu & (= \theta_S)\,. \end{cases} \tag{6-2}$$

Attenuation constant α is expressed as follows;

$$\alpha = \frac{\omega\theta}{2V}\,.\tag{6-3}$$

The constant Q is defined as follows;

$$Q = 1/\theta\,.$$

Logarithmic decrement δ is defined as follows;

$$\delta = \ln \frac{u(x,\,t)}{u(x+l,\,t+T)} = \pi\theta = l\alpha \tag{6-4}$$

where l is wavelength $(2\pi V/\omega)$, T is period $(2\pi/\omega)$.

2) We will assume such a peculiar excitation as expression of displacement $(u(0,\,t))$ at a source is $u(0,\,t) = U\delta(t)$, where $\delta(t)$ means δ-function. The corresponding displacement $u(x,\,t)$ at distance x is given by the following (White [1965]).

$$u = \frac{U}{\pi}\, \frac{\theta x/2V}{(t-x/V)^2 + (\theta x/2V)^2} \tag{6-5}$$

This has hanging-bell-like shape with an single peak (Fig. 6-1). With increase of x, width of pulse becomes broader. The apparent period (T_d) of the displacement pulse (u) shall be tentatively defined as twice of the interval of two points satisfying

$$\frac{\partial^2 u(x,\,t)}{\partial t^2} = 0\,.\tag{6-6}$$

$$T_d = \frac{2}{\sqrt{3}}\, \frac{\theta x}{V} = T_v \tag{6-7}$$

The interval mentioned above ($T_d/2$) also corresponds to the interval between a peak and a trough on wave form of particle velocity ($\dot{u}$). This interval shall be defined as a half of the apparent period (T_v) of $\dot{u}$ (Fig. 6–1).

Particle acceralation ($\ddot{u}=\partial^2 u/\partial t^2$) has two peaks and one trough in its wave form. Interval of the peaks will be defined as apparent period (T_a) of $\ddot{u}$.

$$T_a = \frac{\theta x}{V} \tag{6-8}$$

$$\frac{T_a}{T_v} = \sqrt{3}/2 \doteq =0.87. \tag{6-9}$$

Peak amplitude of u, $\dot{u}$ and $\ddot{u}$ will be expressed as $[u(x)]$, $[\dot{u}(x)]$ and $[\ddot{u}(x)]$ respectively;

$$\left.\begin{aligned}
[u(x)] &= 2\,\frac{U}{\pi}\,\frac{V}{\theta x} & \left(\text{at } t = \frac{x}{V}\right) \\
[\dot{u}(x)] &= \frac{3\sqrt{3}}{2}\,\frac{U}{\pi}\left(\frac{V}{\theta x}\right)^2 & \left(\text{at } t = \frac{x}{V} \pm \frac{T_v}{4}\right) \\
[\ddot{u}(x)] &= 16\,\frac{U}{\pi}\left(\frac{V}{\theta x}\right)^3 & \left(\text{at } t = \frac{x}{V}\right)
\end{aligned}\right\} \tag{6-10}$$

3) Amplitude decays expressed in Eq. (6–10) have not such an exponential character as Eq. (6–1). Attenuation constant α is defined for decay of sinusoidal waves originally. What meaning it has that we observe peak amplitude (apparent amplitude) and apparent period of a pulse-form wave on record? We will compare the amplitudes of two points, ($x-\Delta x/2$) and ($x+\Delta x/2$). As to a sinusoidal wave,

$$\frac{[u(x-\Delta x/2)]}{[u(x+\Delta x/2)]} = \frac{[\dot{u}(x-\Delta x/2)]}{[\dot{u}(x+\Delta x/2)]} = \frac{[\ddot{u}(x-\Delta x/2)]}{[\ddot{u}(x+\Delta x/2)]}$$
$$= e^{(\omega\theta/2V)\Delta x} = 1 + \frac{\omega\theta}{2V}\Delta x + \left(\frac{\omega\theta}{2V}\right)^2\frac{\Delta x^2}{2} + \left(\frac{\omega\theta}{2V}\right)^3\frac{\Delta x^3}{6} + \dots. \tag{6-11}$$

As to the pulse mentioned above,

$$\frac{[u(x-\Delta x/2)]}{[u(x+\Delta x/2)]} = \frac{[x+\Delta x/2]}{[x-\Delta x/2]}$$
$$= 1 + \frac{\Delta x}{x} + \frac{1}{2}\left(\frac{\Delta x}{x}\right)^2 + \frac{1}{4}\left(\frac{\Delta x}{x}\right)^3 + \dots. \tag{6-12}$$

$$\frac{[\dot{u}(x-\Delta x/2)]}{[\dot{u}(x+\Delta x/2)]} = \frac{(x+\Delta x/2)^2}{(x-\Delta x/2)^2}$$
$$= 1 + 2\frac{\Delta x}{x} + 2\left(\frac{\Delta x}{x}\right)^2 + \frac{3}{2}\left(\frac{\Delta x}{x}\right)^3 + \dots. \tag{6-13}$$

$$\frac{[\ddot{u}(x-\Delta x/2)]}{[\ddot{u}(x+\Delta x/2)]} = \frac{(x+\Delta x/2)^3}{(x-\Delta x/2)^3}$$

$$= 1 + 3\frac{\Delta x}{x} + \frac{9}{2}\left(\frac{\Delta x}{x}\right)^2 + \frac{19}{4}\left(\frac{\Delta x}{x}\right)^3 + \ldots \tag{6-14}$$

In the whole above series, $(\omega\theta/2V)\,\Delta x < 1$ and $\Delta x/x < 1$ have been assumed.

We will find the value of ω of a sinusoidal wave which has the same amplitude decay as the pulse, between $(x-\Delta x/2)$ and $(x+\Delta x/2)$. Such a sinusoidal wave will be called the equivalent sinusoidal wave.

As to displacement, we compare Eq. (6-12) and Eq. (6-11). To make both amplitude ratios equal, the following relation must be satisfied,

$$\frac{\Delta x}{x} = \frac{\omega\,\theta\,\Delta x}{2V}. \tag{6-15}$$

Error of amplitude ratio (ε_d) due to neglection of higher order term in the series is given by

$$\varepsilon_d = -\frac{1}{12}\left(\frac{\Delta x}{x}\right)^3$$

If the value of ω satisfying Eq. (6-15) is denoted as ω_d',

$$\omega_d' = \frac{2V}{x\theta} = \frac{4}{\sqrt{3}}\frac{1}{T_d}$$

$$T_d' = \frac{2\pi}{\omega_d'} = \frac{\pi\sqrt{3}}{2}T_d = 2.72\,T_d \tag{6-16}$$

As to particle velocity, Eq. (6-13) and Eq. (6-11) are compared.

$$\left. \begin{aligned} \omega_v' &= 2\,\omega_d' \\ T_v' &= \frac{2\pi}{\omega_v'} = \frac{\pi\sqrt{3}}{4}T_v = 1.36\,T_v \\ \varepsilon_v &= -\frac{1}{6}\left(\frac{\Delta x}{x}\right)^3 \end{aligned} \right\} \tag{6-17}$$

As to acceleration,

$$\left. \begin{aligned} \omega_a' &= \frac{6V}{\theta x} = \frac{6}{T_a} \\ T_a' &= \frac{2\pi}{\omega_a'} = \frac{2\pi}{6}T_a = 1.05\,T_a \\ \varepsilon_a &= -\frac{1}{4}\left(\frac{\Delta x}{x}\right)^3 \end{aligned} \right\} \tag{6-18}$$

In the above expression, $\omega_v{'}$ and $\omega_a{'}$ are the values of ω of the sinusoidal waves, which have the same amplitude decay as the velocity pulse and the acceleration pulse respectively, as well as $\omega_d{'}$ as to the displacement pulse. ε_v and ε_a are errors born by neglecting higher order of series, as well as ε_d.

From Eq. (6–17) and Eq. (6–18), it is concluded that the decay of peak amplitude of the velocity and acceleration pulses is equal to that of an equivalent sinusoidal wave, whose period is nearly equal to apparent period of the pulses observed at the middle point (x) of two observation points.

Also for the displacement pulse (u), application of the same description is formally possible, by modifying definition of apparent period T_d, though descrepancy between $T_d{'}$ and T_d is large as shown in Eq. (6–16). However, this has little meaning from practical point of view because it is difficult to indicate an interval of such a nonoscillatory pulse as u on actual records. Hence, analytical description for u is only for reference. With increase of distance x, the period of such an equivalent sinusoidal wave becomes longer and the amplitude decay becomes smaller (Fig. 6–1).
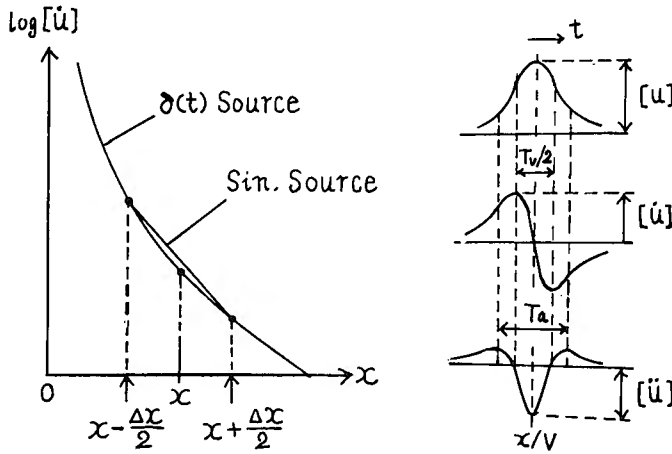
Fig. 6–1.   Explanation of attenuation.

With increase of order of time derivative as to the pulse, period ($T_v{'}$, $T_a{'}$, etc.) of the equivalent sinusoidal wave becomes equal to the apparent period (T_v, T_a, etc.) of the pulse, with better accuracy. Increase of order of time derivative makes the wave form more oscillatory.

Predominant frequency should be indicated on a spectrum chart, in strict meaning. This word used in 4–2 (*3*) is one for convenient sake. It means that the apparent one measured as to a wave train on record. Error due to this is not so important in that step of discussion.

(2)   *Effect of predominant period of source*

1)   In real case, displacement wave form at a source is not δ function, it will

be broader impulse or oscillatory pulse with some duration. Usually, actual wave form of particle velocity is oscillatory. It has a predominant frequency even at a source.

In order to make the condition simple, we regard that the wave form at a real source can be represented by one of the pulses at distance x_o, radiated from the δ function type source. By applying Eq. (6–7) and (6–8), distance corresponding to the predominant period (apparent period) can be obtained. Hence, amplitude decay of δ function type source can be applicable also to the above case, if real distance x is replaced by $x+x_o$. x_o shall be named the "equivalent distance of a source".

As an example, acceralation wave form shall be considered.

$$V T_a = \lambda_a \tag{6-19}$$

λ_a is wavelength corresponding to T_a. (Suffix "a" is omitted in the following.) From Eq. (6–8)

$$\lambda = \theta x \tag{6-20}$$

If $x+x_o$ is conducted into Eq. (6–20),

$$\lambda = \theta \, (x_o + x)$$
$$= \lambda_o + \Delta \lambda \, ,$$

where

$$\lambda_o = \theta x_o = V T_o$$
$$\Delta \lambda = \theta x \, . \tag{6-21}$$

λ_o and T_o are apparent ($\doteqdot$ predominant) wavelength and period of a source respectively. $\Delta \lambda$ means variation of apparent wavelength through propagation distance x.

2) In the case of a spherical wave radiated from a point source, $1/x$ should be multiplied to the expressions for the amplitude mentioned above. Of course, near field terms are neglected here. There is no need of modification for period and wavelength.

3) Average value of λ_o for a source produced by an explosion of a single cap is about 3m as observed in Fig. 4–6. Hence $\Delta \lambda = 0.3$m shall be assumed for tolerable error. Logarithmic decrement is $0.2-0.005$, according to White, which is conformable with the author's data (Table 6–1). This value shows wide variety depending on types and conditions of rock. Using Eq. (6–4) and Eq. (6–21),

$$x = \frac{\pi \Delta \lambda}{\delta}$$

$$\doteqdot \begin{cases} 5\text{m, at } \delta = 0.2 \\ 180\text{m, at } \delta = 0.005. \end{cases}$$

For the measurement of predominant period of the source, the wave observation should be done at the distance less than such x (safty distance). The safty distance depends very strongly on rock condition.

(3) *Measured values of logarithmic decrement*

The author measured attenuation characteristics of rock at some places by analyzing peak amplitude (usually peak to peak) and apparent period based on the idea mentioned above. The data are rather poor in quality and number. Much measurement should be done with sufficient accuracy to conclude comprehensive conclusion. The author's data are shown in Table 6-1. The values are conformable with data gathered by White (see Fig. 3-9 in his text book [1965]).

Table 6-1.   Measured data as to attenuation

place	rock	velocity (km/s)		experi- ment	δ	
		V_P	V_S		P	S
Sazare Mine	quatz shist (paleozoic)	6.4		1962	$0.02 \pm 100\%(3.2)$	
Makimine Mine	black phyrite (mesozoic)	5.5		1961	$0.38 \pm 10\%$ (6.1)	
//	//		3.7			$0.07 \pm 50\%$ (9.3)
Myoho Mine	sand stone (tertiary)	3.1		1960	$0.34 \pm 50\%$ (4.3)	
//	//	3.0	1.9	1957		$0.16 \pm 50\%$ (6.3)

(   )   wavelength [m]
        No rocks are suffered by remarkable fractuation.

7. S wave logging

7-1 Significance of S wave logging

Logging is to take some data along boreholes. As well as general logging techniques, S wave logging is also done to measure physical properties in the ground, exactly and in detail.

Significance of S wave study itself has been discussed in introduction, and will considered again in Section 10 as to some restricted subjects. Hence, this is not specified here.

In order to explore seismic characteristics under the ground, the refraction method is usually applied. Recently refraction survey by SH wave has become popular in Japan. However, necessary informations for some purpose are not always obtained by such a seismic work on the ground surface. This is more severe in the S wave than in the P wave by the following reasons.

a) Analysis of refraction surveys are based on such an assumption as wave velocities are higher in deeper layer.

Velocity variation between every layers is larger in the S wave than in the P wave. Sometimes there are such abnormal case as S wave velocity decreases in deeper

layer.

If soil layers are not saturated by water, tendency of velocity variation is the same for both the P and S wave approximately. As discussed in Section 9, variation of P wave velocity becomes smaller, if soils are saturated with water. S wave velocity, however, is nearly free from effect of water-saturation.

b) As to SH refraction survey, maximum length of the geophone spread is restricted by limit of source energy, which is supplied by human power and some kinds of mechanical and explosion source. As to the human power, the maximum length is usually about 100m. Other kinds of the source allow that length to increase 2-3 times, in favourable conditions. Maximum depth explored by the refraction surveys is usually less than 1/3 of spread length.

c) Identification of the S wave (especially its first kick) is sometimes difficult in the refraction survey. Hence, accuracy of analysed results becomes lower. Identification of the S wave becomes easy and the accuracy of measurement increases, by inserting either detectors or a source, or both in a borehole.

7-2 Review of several logging method as to S wave

(1) *Source in a borehole and geophones on ground surface*

This is the simplest method. As discussed in Section 4, the S wave can be generated by a small explosion. This method had the following characters and difficulties.

a) Generation of the S wave by a small explosion is difficult in granular soils having larger grain-size (for example, larger than 3–5cm).

b) Angle (measured from hole axis) giving maximum radiation amplitude is expected about 45° as discussed in Section **4**. Necessary length of geophone spread is nearly equal to shot depth. The geophone spread on the surface should be set in radial direction from the top of the borehole.

c) Since propagation with sufficient energy along hole axis can not be expected, analysis of the velocity distribution needs some assumption to simplify the conditions.

d) Practice of this method is very simple. Specialized equipment is not required.

e) Usually in this practice, geophones spread is fixed, and explosions are repeated at every source position, one by one.

(2) *A source on ground surface and geophone in a borehole*

By putting a source on the ground surface, we can have freedom to select favourable kinds of the source. The clamped borehole geophones specified in Section **3** are also used for this purpose. Recently this method has been spreading in Japan, since the author tried this method in 1966 (Kitsunezaki [1967]). This method has following characters. Usually, S wave logging means this method.

a) S wave propagating along borehole is measured, by employing SH type source discussed in **4-3**. Accuracy of analyzed result becomes higher than the method of *(1)* in general.

b) Operation of a borehole geophone needs some techniques. Installation of the geophone is difficult at layer loosened severely.

c)   Usually in this method, the source is fixed and installation position of a borehole geophone is moved along the hole axis.

d)   Maximum depth of the survey is about 100m, as far as human power is used for SH type source.

e)   If the site favours wave conversion, from P to S, an explosion source can be used. It is interesting that efficiency of wave conversion seems to be higher at the interface covered with liquid-like surface layer, where the SH source is not effective.

f)   Direct SV wave generated by an explosion can be applicable sometimes. Effective radiating direction is oblique to hole axis (vertical). This source is favourable for deeper survey in certain condition.

(3)   *Both a source and geophones in a borehole*

1)   Detailed measurement can be practised by a small scaled spread (several meters) consisting of a source and geophones. By inserting such a spread in a borehole, complete logging can be done. This idea itself is the same as P wave logging. In practice, however, there are some difficulties to be solved.

In order to assure normal detection of the S wave, detectors must be fixed every positions. The same mechanism as the clamped borehole geophone can be applied in its principle. However, development of some practical technique is necessary to construct practical probe consisting of a source and detectors. A trial for the source has been introduced in Section **4**.

2)   Logging tool of this type will find a wide application field in a survey of a deeper place. In shallower depth, the method of (2) may be simpler and accurate enough for usual purpose of survey.

In real field sometimes, conditions of ground surface are not so favourable for installation of the source. And sometimes near the ground surface we have such a unfavourable media condition that the effective transmition of the S wave is obstruted. This condition is provided by crushed or weathered rock surface, very liquid-like soil layer, gravel layer with large grain size and paved ground, etc..

The complete logging tool discussed above shall be applicable also in those area. It is used also in irregular media, where horizontal bedding is not assured. Usual rocks in tunnels and dam site are such cases.

3)   The complete logging tool will require somewhat troublesome techniques and much time. It should be also considered to use indirect logging methods as supplementary means, discussed in the next section. S wave velocities can be deducted from tube wave velocities or data of resistivity log.. Those indirect methods are very easy in practice and need less time than direct methods.

For example, economical and still useful survey of engineering seismology for rather large area will be accomplished by combining the direct and indirect methods effectively.

8. Indirect method for S wave velocity logging

8-1 Tube wave logging

(1) Pressure wave along a liquid column surrounded by solid is called the tube wave (White [1965], Kitsunezaki [1968]). The tube wave is sometimes called the borehole wave. In this paper, "B" is used as a symbol denoting this wave.

(2) An elastic constant (K_B) defined as the ratio of axial stress to axial strain of a liquid column is affected by elasticity (β) of solid wall. The elasticity of solid wall are represented by rigidity (μ) alone in infinite homogeneous media. Namely, at sufficiently low frequency, propagation velocity (V_B) of this wave is given by the following.

$$V_B = \sqrt{\frac{K_B}{\rho_w}} \tag{8-1}$$

$$\frac{1}{K_B} = \frac{1}{\kappa_w} + \frac{1}{\beta} \tag{8-2}$$

$$\beta = \mu \qquad \text{(infinite homogeneous solid).} \tag{8-3}$$

where κ_w and ρ_w are bulk modulus and density of the liquid in a borehole. By the above relations, rigidity of solid media can be evaluated from V_B observed.

(3) At higher frequency, V_B shows dispersive characteristic (Biot, [1952]). From practical point of view, attention should be paid to condition giving constant velocity. According to Biot's analysis, if the condition, $\Lambda_B > 5d$, is satisfied, V_B is sufficiently constant. In this expression, l_B is wavelength of the tube wave, d is diameter of the borehole. The author's experiments are intended to satisfy such a condition.

(4) Eq. (8-1), Eq. (8-2) and Eq. (8-3) can be replaced by the following expression.

$$V_B = \frac{V_S}{\sqrt{\rho_w/\rho + (V_S/V_w)^2}} \tag{8-4}$$

where, V_S and ρ are S wave velocity and density of the solid. ρ_w is density of liquid. This relation is shown in Fig. 8-1.

Eq. (8-4) is an expression for V_B in infinite homogeneous solid.

(5) There is a theoretical difficulty of the existance of the tube wave, if the condition, $V_B < V_S$, is not assured. As far as Eq. (8-4) is applied, the tube wave can not exist in such medium, as V_S is lower than 1.1—1.3km/sec (see Fig. 8-1). Under the condition, $V_B > V_S$, theoretical treatment is complicated, and the numerical solution has not been obtained. At least, the tube wave, characterized as one di-
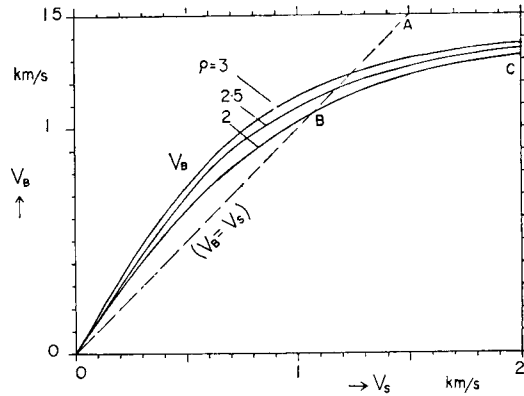
Fig. 8-1. Relation between V_B and V_S, under assumption of $\rho_w = 1$ g/cm^3

mensional boundary wave without attenuation, can not exist. In this case the tube wave will be modified to a wave, to which Eq. (8-4) is also applicable in lower frequency, and its attenuation becomes larger with increase of frequency.

(6) Many experiments on the tube wave have been carried out, in rocks and soils. Experimental results show that a liquid wave like tube wave usually exists, and that its velocity is usually lower than V_S of surrounding solid. In soils, which are also characterized by low V_S, attenuation of the wave is hgih. This wave, however, is sufficiently predominant to be clearly recorded in any place along a borehole.

The author thinks that high attenuation in lower V_S media is not due to energy radiation, from the water to the solid (by reason of $V_B < V_S$), but departure of media conditions from ideal ones. This departure means existance of such factors, as friction due to roughness of the wall, viscosity of the liquid (thick mud), water-permeability of the wall, and inelastic characteristics of the solid, etc..

Such a liquid wave shall be also called the tube wave. There is no reason to distinguish this from ideal tube wave, from practical point of view. Essential meaning of a tube wave is that the wave is liquid wave whose velocity is affected by μ in the solid.

(7) Results of the field-experiments are shown in Fig. 8-2.* From Fig. 8-2 we can know relation between real V_S and V_S (defined as V_S') evaluated by Eq. (8-4). In this evaluation, V_B is observed one, ρ is measured or assumed one. ρ_w is assumed $1 g/cm^3$ in the whole cases. Solid media applied in Fig. 8-2 are a rock and many kinds of soils. The soils are clay, silt, sand and gravel, of alluvium and diluvium. From Fig. 8-2, the following relation is conducted as empirical one.

$$V_S'/V_S = 0.53 \qquad (8-5)$$

* In Fig. 8-2, some data are added to the data in the author's previous paper [1968], and a datum in the latter has been corrected here based on later experiment. A datum obtained by the Oyo-chishitsu Co. is also plotted here.
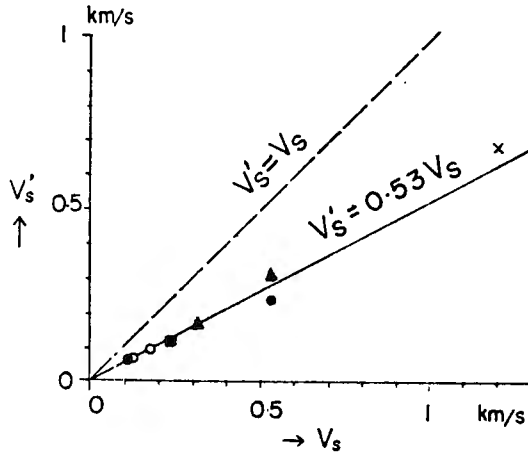
Fig. 8-2. Experimental results showing relation between S
wave velocity (V_S) and the one ($V_{S'}$) evaluated by Eq. (8-4).

Such a simple relation allows to estimate V_S (or μ) from V_B observed.

(8) $V_S' < V_S$ is explained by assuming that rigidity of media near the wall surface
is lowered. Apparent rigidity corresponding to V_S' is denoted $\mu'(\mu' = \rho V_S'^2)$. The
expression of corresponding to Eq. (8-5) is

$$\mu'/\mu \doteqdot 0.3 .\tag{8-6}$$

The author [1968] evaluated μ'/μ considering a model of two walls coaxially layered
around the borehoe [Fig. 3-9 (b)]. It needs considerable decrease of the rigidity to
explain Eq. (8-6). If thickness of the inner layer is the same as hole diameter, Ex-
pression for necessary μ_1/μ is

$$\mu_1/\mu \doteqdot 0.2 ,\tag{8-7}$$

where μ_1 and μ are rigidities in inner and outer layer respectively. If the inner layer
is sufficiently thick,

$$\mu_1 = \mu' \qquad \text{(by definition of μ').}$$

If there is really such considerable decrease of rigidity in near-surface, it should be
noted that the ratio of decrease observed (corresponding to Eq. (8-5)) is rather too
constant. There may be certain regular decreasing process behind the fact.

    This rigidity decrease can not be explained as that due to stress release on hall
wall. For example, Hardin's relation [1963] as to dependency of V_S on pressure P is

$$V_S \propto P^n \tag{8-8}$$

where $n = 1/3 - 1/4$. If P is evaluated as the mean of three principal stresses, the
pressure (defined as P') on the wall after hole opening is not less than 70% of original
one (P). If S wave velocity corresponding to P' is named V_S', $1 \geq V_S'/V_S \geq 0.9$, where

V_S is S wave velocity at a place free from effect of hole opening.

The author can not give complete explanation on constant ratio of V_S' to V_S. Velocity decrease itself near hall wall may be due to inelastic disturbance by hall opening.

In order to practise tube wave logging, the empirical relation between V_S' (or V_B) and V_S is the most fundamental one. This relation must be made concrete by a sufficient number of data. At present the author can say only that tube wave logging is empirically favourble as one of the indirect S wave loggings. White [1965] also carried out measurement of V_B for estimation of V_S. However, he did not pay attention to difference between V_S' and V_S.

(9) *Logging tool for tube wave*

Tube wave can be easily generated by explosion of a cap. Earliar data were obtained by this method. More elegant source was designed by the author whose mechanism is the solenoid hammer explained in Section 4. Principle of the source is shown in Fig. 8–3. Kinetic energy of the hammer at impulsion is about 4 joule. One record is obtained by one shot. Syncroscope equiped with a *polaroid* camera is used as a recorder.
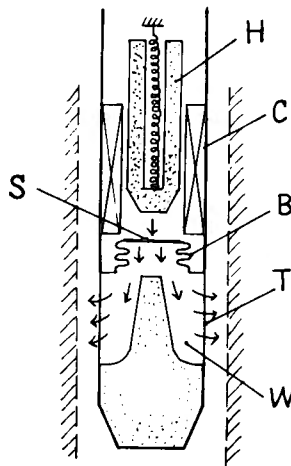
Fig. 8–3. A source for tube wave and P wave.
S : radiating plate
B : bellows
T : rubber skin
C : solenoid
H : hammer
W : water contained

Example of record is shown in Fig. 8–4. In Fig. 8–4 depth of the source is fixed, and the detector (hydrophone) is moved to every depths for the observation. Propagation of predominant tube wave B can be observed with the P wave. In usual logging, a pair of two hydrophones are hanging with the source. With fixed intervals

Fig. 8–4.   Record showing tube wave and P wave.

(2m respectively), this spread is moved along a hole. P wave data also can be obtained by the same tool.

8–2   Resistivity logging

(*1*)   The author thinks that the most important factor of media controlling V_s in granular soils is void ratio.   Hardin's experiment [1967] supports this idea. According to him, V_s is governed by void ratio (*e*) and confining pressure (*P*), as far as its fundamental feature.

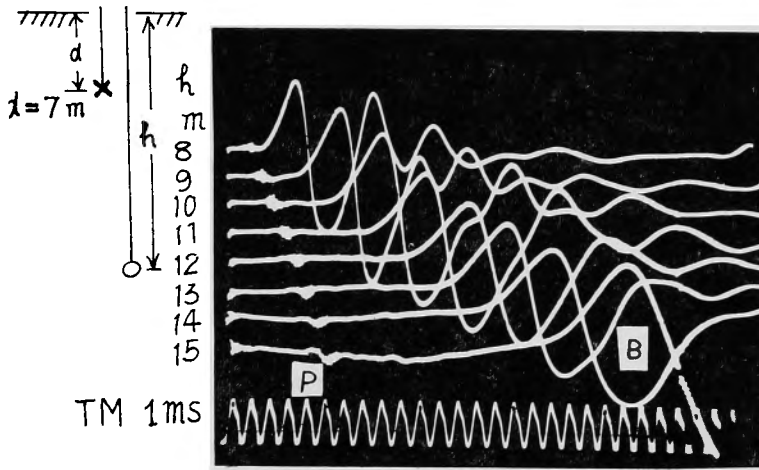(*2*)   Void ratio can be estimated to some degree by analyzing resistivity log data. In conventional operation of resistivity log, measurement is done for two interval (short and long) of poles, at least.   From the combination of data obtained at different intervals of the poles, resistivity of media near hole (mud invasion region (R_i)) and of mud (R_m) is evaluated by using standard departure curves (Shulumberger Well Survey Corp. [1949]).   Usually, the following relation is applied for estimation of porosity

$$F \equiv \frac{R_i}{R_m} = A\phi^{-\nu} \tag{8–9}$$

where ϕ is porosity, ν and A are constants. F is called the formation factor.

(*3*)   The author has carried out resistivity logging, mainly by the two-pole method (Yamaguchi [1963]).   In some places, V_s logging was simultaneously practised.   Relation between R_i/R_m and V_s is shown in Fig. 8–5.

The data are obtained in depth of 10—50m.   Observed values of V_s are normalized to ones at 2 bar of vertical effective pressure (*P*) assuming $V_s \propto P^{1/4}$.   Soils applied in this figure are sand and gravel, of alluvium and diluvium.   Correction of void ratio (*e*) due to depth is not considered.   According to Hardin, effect of pres-

sure on variation of e is not important in sand.
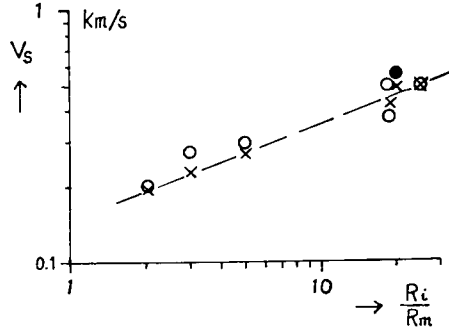
This results suggests regular relation between them.

Fig. 8-5. Experimental relation between V_s and R_i/R_m.

○ V_s values directly measured.

● V_S evaluated from observed V_B by applying the correction of Eq. (8-5).

×   normalized values obtained by correcting the above values to the state of 2 bar.

As to ν and A, there are some experiments.

Yamaguchi [1963] carried out many measurements on various kinds of granular soils in Japan. According to him

$$\nu = 2.5 , \qquad A = 0.43 . \tag{8-10}$$

By applying Eq. (8-9), relation between V_s and R_i/R_m is modified to one between V_S and e $(e = \phi(1-\phi)^{-1})$. This is shown in Fig. 8-6. Values of V_S shown in this figure are normalized to the values at pressure of 2 bar.

For reference, classical relation obtained by Archie [1942] is shown in Fig. 8-6. According to him,

$$\nu = 1.3 , \qquad A = 1 \tag{8-11}$$

for unconsolidated sand.

There is large discrepancy between values deducted by Archie and ones by Yamaguchi. e by Archie's formula shows too small value, in larger range of R_i/R_m.* Soil tests were done by Osaka Doshitsu-Shikensho (Soil Test Laboratory) for boring sample obtained at a site near the place, where a datum at extreme right in Fig. 8-5 (at extreme left in Fig. 8-6) was obtained. According to this, e in the corresponding

---

* Yamaguchi's relation is based on laboratory experiment for samples of unconsolidated granular soil in which $\phi = 0.3 - 0.5$ $(e \doteqdot 0.4 - 1.0)$. In this paper, it is assumed that his relation is available in wider range of ϕ over its original range. In Archie's paper, available range of ϕ for the present case is not shown.

layer (gravel) is 0.23—0.35. Therefore, Yamaguchi's formula is considered to be more conformable with soils in the author's experiment and adopted in the succeeding discussion.
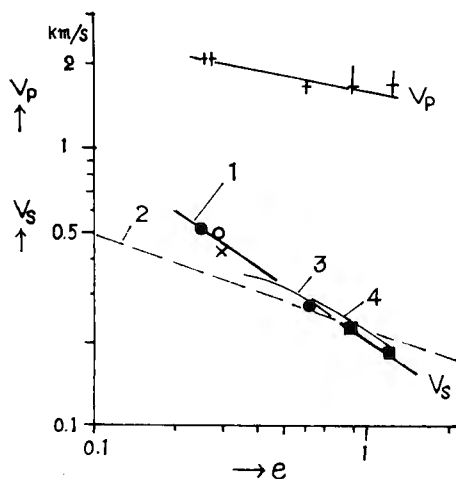

Fig. 8–6. Relation between V_S and e deduced from R_i/R_m.

1 $R_i/R_m = 0.43 \, \phi^{-2.5}$ (by Yamaguchi) $\Big\}$ evaluation of e
2 $R_i/R_m = \phi^{-1.3}$ (by Archie)

3 round sand $\Big\}$ Hardin's relation ($V_S : e$)
4 crashed sand

Hardin's relation at the same pressure (confining pressure) is also shown in Fig. 8–6 for comparison. His relations cited here are for sand subjected by effective pressure $P=2$ bar at water-saturated condition. These relations at water saturated condition were deduced by the author from Hardin's relation given for dry condition, applying Gassmann's formula. Pressures in Hardin's experiments are confining pressure (in dry condition) and pressures in the author's experiment mean vertical component of effective pressure. If the average of effective principal stress is to be corresponded to the former, V_S is the author's experimental relation may be made higher by about 10%, in order to compare with Hardin's relation. In the present accuracy of discussion, however, such a consideration is not so important. We should rather pay attention to good agreement between both. (V_S ; R_i/R_m) relation is more important than (V_S ; e)*, as far as the evaluation of V_S from resistivity log is concerned.

In order to make (V_S ; R_i/R_m) relation confirm, much data should be gathered.

(4) Resistivity logging for the present purpose, has not meaning in clay. This method based on the assumption that only both water content and its resistivities are key factors governing resistivities of media, and that water contained in media

* (V_S; e) means relation between V_S and e.

near the hole is completely replaced by the mud water in the hole. The above condition can be satisfied only by such granular soils, as sand and gravel. If content of clay in soils is a little, clay may be regarded as something like void water (mud). Usually V_S of clay is lower than that of sand. Considerable error will not be introduced into evaluation of V_S, even if a little of clay is regarded as liquid.

Resistivity log data are analyzed by using Shulumberger's "standard departure curve" [1949]. In order to get good results by this method, the granular layers analyzed must be seated between two clay layers, and then resistivity of the granular layer must be homogeneous. In practical analysis, of course, unimportant scatters of resistivity in the layer is averaged.

For the above reason, the state of soil to which this method can be applied is restricted. Hence, this method is less comprehensive in its fields applicable than the tube wave method to obtain S wave velocities. In Japan, resistivity logs are not quantitatively analyzed, but qualitatively, except oil prospecting and particular surveys in water well.

However, since resistivity logging is very popular in field of water well, soil survey, and oil prospecting, if the resistivity loggings practised at present are normalized under certain standards, large amount of data as to V_S distribution under the ground will be obtained. The resistivity logging are easily practised also in deeper place. This provides a supplementary method for wide regional survey of the ground condition.

8–3   Other indirect methods for S wave velocity logging.

There are several kinds of radioactivity logging, by which water contents and densities of soils can be detected. They provide more direct data for porosity. Hence, such logging should be studied in connection with S wave velocity. This belongs to future problem.

P wave velocity has also some relations with S as will be discussed in the following section. Velocity variation of P wave in water-saturated soil is rather smaller than that of S. But P wave velocity can be measured more easily and with higher accuracy than S, if a proper logging tool is applied. By this reason, more attention should be paid to relation between P and S wave logging.

Lastrico [1970] discussed relation between S wave velocity and many kinds of logging data, including density and P wave velocities, and applied the relation to evaluation of V_S distribution for purpose of engineering seismology.

Soil tests for borehole sample also serve as one kind of logging for V_S determination.

9. S wave velocity

9–1 Seismic velocities in soils

(1) Roughly speaking, there is the following relation in S wave velocities of soils in general (for erample, Ohta [1968], Doboku-buttan-kenkyu-kai [1970]).

$$V_S \text{ (gravel)} > V_S \text{ (sand)} > V_S \text{ (clay)}.$$

discrepancy of V_S in gravel and sand can be understood as differnece of void ratio e.

e may be also one of the most important factors controlling V_S of clay. However, physical process giving V_S may be more complicated in clays than in sands, as expected from general dynamic characteristics in soil mechanics (Telzaghi [1948]). At present, the author can not say much about the problem of V_S of clay.

As to clay, undisturbed soil samples can be taken in boreholes, and hence usual test methods of soil mechanics can be applied to these samples as well as measurements of V_S in laboratory. Research of key factors controling V_S in clay may be successfully developed by this approach, if sound connection between laboratory and field measurements of the S wave is introduced into it.

However, in sand and gravel, it is difficult to take undisturbed samples. Hence, the physical logging mentioned above (tube wave, resistivity, radioactivity) has enough meaning to be applied to sand and gravel in order to find essential factors governing V_S. Such a in situ mechanical tests as standard penetration tests and lateral load tests also have supplementary meaning for determination of V_S. By the reason mentioned above, the whole side of researchs and surveys of the S wave should be carried out under two large divisions, namely clay and granular soils.

(2) Soils are not ideal elastic material, and hence, its dynamic properties depend also on magnitude of strain. However, if strain is less than 10^{-6}, seismic velocities are considered to be sufficiently constant (Seed, [1969]). In the discussion in this paper, it is presupposed that strain is sufficiently small to neglect strain effect on S wave velocities. Such presumption is not contradict the field-experiments of seismic waves, in which strain is usually less than 10^{-6}.

9–2 Seismic velocities in granular soil

(1) In this section, general characteristics of seismic wave velocities in granular soils will be discussed. The author's experimental relation in Fig. 8–6 is $(V_S \, ; e)$ relation in water-saturated soils. Assuming that this relation is generally hold, $(V_S \, ; V_P)$ relation under saturated and dry condition shall be deduced.

(2) In these evaluations Gassmann's formula [1951 a] is applied. Following Gassmann, the notations shall be defined as follows;

$V_P, V_S, \rho,$ etc   : quantities of a water-saturated system consisting
                                              of water and framework.

$\hat{V}_P$, $\hat{V}_s$, $\hat{\rho}$, etc. : quantities of a grain particles itself.

$\bar{V}_P$, $\bar{V}_S$, $\bar{\rho}$, etc. : quantities of a framework only (system of dry condition).

$\tilde{\kappa}$, $\tilde{\rho}$, etc. : quantities of water filling void.

κ=incompressibility.

Gassmann's formula is applicable not only to granular soils, but to all kinds of porous media having effective pores. In his formula, it is assumed that the liquid filling void does not affect μ, but κ. Hence,

$$\mu = \hat{\mu} .$$
(9–1)

κ is given by the following equation.

$$\left. \begin{aligned} \kappa &= \hat{\kappa} \, \frac{\bar{\kappa} + Q}{\hat{\kappa} + Q} \\ Q &= \frac{\tilde{\kappa}(\hat{\kappa} - \bar{\kappa})}{\phi(\hat{\kappa} - \tilde{\kappa})} \end{aligned} \right\}$$
(9–2)

And then

$$\left. \begin{aligned} \rho &= \phi \tilde{\rho} + \bar{\rho} \\ \rho &= (1 - \phi) \, \hat{\rho} \\ V_P &= \sqrt{\frac{\kappa + 4\mu/3}{\rho}} \\ V_S &= \sqrt{\frac{\mu}{\rho}} . \end{aligned} \right\}$$
(9–4)

Effective porosity, ϕ, is replaced by e;

$$e = \phi/(1 - \phi) .$$
(9–5)

(3) κ and V_P shall be evaluated through the following processes.

a) The relation between e and V_S in Fig. 8–6 is assumed to have general applicability.

b) $\bar{V}_P/\bar{V}_S = \sqrt{3}$ is assumed under any condition.

c) Main part of grains in granular soils consists of silicious minerals. The following quantities are assumed.

$$\hat{\kappa} = 36 \times 10^{10} \text{ dyne/cm}^2$$
$$\hat{\rho} = 2.57 \text{ g/cm}^3$$

And then, as to water,

$$\tilde{\kappa} = 2.25 \times 10^{10} \text{ dyne/cm}^2$$
$$\hat{\rho} = 1.0 \text{ g/cm}^3$$

d) It is assumed that only elastic constants of the framework are affected by pressure. Following Hardin's experiments, the assumed relation is
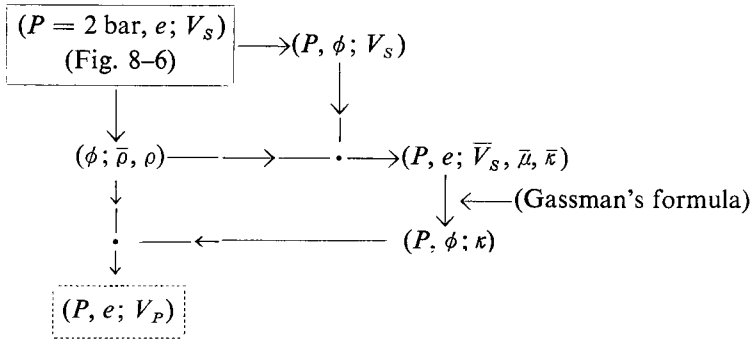
$$\bar{V}_s = C P^{¼} .$$

$$V_s = C \sqrt{\frac{\bar{\rho}}{\rho}} \, P^{¼} = \sqrt{\frac{\bar{\rho}}{\rho}} \, V_s , \qquad (9\text{-}6)$$

where P is effective pressure ($=$total pressure$-$pore water pressure) at water-saturated condition. C is a proportional constant.

e) Variations of e and $\hat{\rho}$ by pressure are neglected (Hardin's experiment supports this).

f) Calculation process is as follows,

$$
\boxed{\begin{array}{c} (P = 2\ \text{bar}, e; V_s) \\ (\text{Fig. 8-6}) \end{array}} \longrightarrow (P, \phi; V_s)
$$

$$(\phi; \bar{\rho}, \rho) \longrightarrow \cdot \longrightarrow (P, e; \bar{V}_s, \bar{\mu}, \bar{\kappa})$$

$$\downarrow \longleftarrow (\text{Gassman's formula})$$

$$\longleftarrow (P, \phi; \kappa)$$

$$\boxed{(P, e; V_P)}$$

The results obtained are shown in Fig. 9-1. From the curves we can know that the variation of V_P due to pressure change is very small for the soils with larger e, and somewhat larger for the soils with smaller e. V_s is rather affected by pressure than V_P.

If the soils are dry, $V_P = \sqrt{3}\, V_s$. Proportion of variation of V_P due to pressure is the same as V_s. Hence the curves for V_P in the dry soils are omitted in Fig. 9-1.

(*4*) V_P values obtained simultaneously with the experiment of V_s are normalized to the values for $P=2$ bar and plotted in Fig. 8-6. This V_P curve is the same as the V_P curve for $P=2$ bar in Fig. 9-1. Most of the data are obtained by the method explained in (2) of 7-2. The accuracy of V_F measurement is low due to its high velocity characteristics, because the special logging tool for V_P was not employed, except a few data. Ranges of errors are shown by length of bar. For complete discussion of V_P, a lot of more accurate data are needed.

Many measurements have been done for V_P, sometimes with V_s, of soils in Japan. The data available for the present discussion are very few because of insufficient accuracy of V_P values and of lack of the related physical data (densities, void ratios and water contents).

(*5*) In the previous discussion, $\bar{V}_P = \sqrt{3}\, \bar{V}_s$ is assumed for dry granular soils, as well as in usual hard rocks. The author thinks that several experiments and theo-
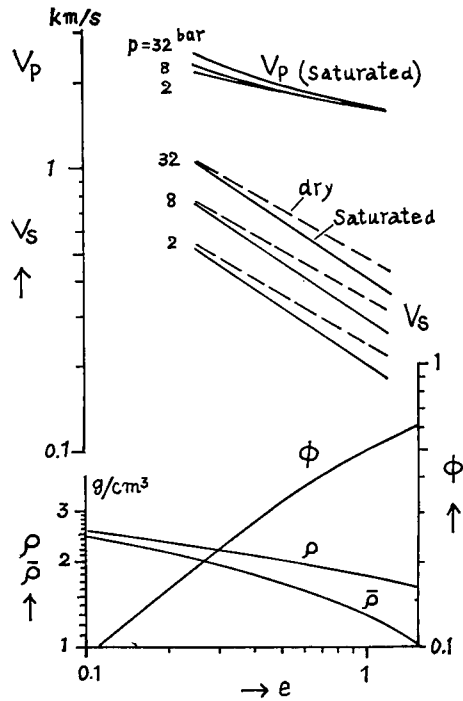
Fig. 9–1. V_P and V_S in different conditions deduced
from $(e \ ; \ V_S)$ relation of Fig. 8–6.

retical considerations support the fact $\overline{V}_P \fallingdotseq \sqrt{3} \ \overline{V}_s$. For example,

a) Hardin's laboratory-experiments [1963],

b) White's field-experiments (Fig. 2–15 in his text book [1965], [1953], for example),

c) theoretical study of model of sphere packing (Gassmann [1951 b]),

d) the author's field experiment (see Fig. 5–2 (b), for example).

The direct experiment of this in field is not so easy by the following reason.

a) In usual conditions of Japan, thickness of dry layers is too thin to measure velocities with sufficient accuracy.

b) There are wide variations of properties of the soils in shallow depth, due to weathering effect, recent sedimentation, and water content.

c) Since attenuation of P wave is very large in dry soils such a logging tool as referred in (9) of 8–1 is not so powerful to produce measurable P wave motions.

Hence, some practical devices are needed to obtain accurate data, depending on individual field conditions.

9–3 Variation of velocities in granite accompanied by weathering effect.

(1) Based on the field-experiments, the author [1965] discussed variation of

velocities in granite accompanied by weathering effect and he presented the empirical relation between V_F and V_S as follows (Fig. 9–2);

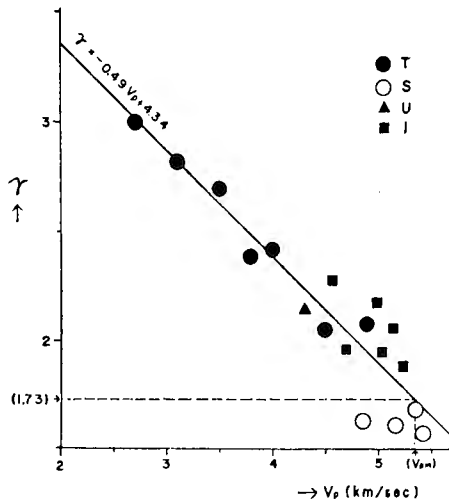$$\frac{V_P}{V_S} = -0.49\, V_P + 4.34\,.\qquad(9\text{--}7)$$

Fig. 9–2. Variation of V_P/V_S in granite due to weathering and fracturing. The whole data except "S" were obtained by field test.
$\gamma = V_P/V_S$

Most of the data in the above were obtained in adits of a power plant site near Tsuruga, Japan. Depth of the places, where data are obtained are 20m below the mean sea level and about 25—70m below the ground surface. And the site is situated at sea coast. Therefore, the data obtained are considered to be ones in condition of water-saturation. In this case effective pressure is less than 14 bar. Increase of $\overline{V}_P$ and $\overline{V}_S$ by this pressure is considered to be less than 10%. (See Matsushima [1960] and Honsho [1966], for example.) Therefore, in the following discussion, the above relation is regarded to mean the relation under condition free from pressure.

(2) Recently, Kunori, Abe and Saito [1970] carried out systematic laboratory tests for granitic rock samples, under dry condition free from external pressure.

(3) Their relations are compared with the author's one, through the following steps.

a) The curves representing mean characteristics of the scattered points ($\overline{V}_S$) in Fig. 9–3 (b) are assumed by the author as the curves shown in this figure.

b) To make simple, $\overline{V}_P/\overline{V}_P = \sqrt{3}$ is assumed. The curve of $\overline{V}_P$ corresponding to this is shown in Fig. 9–3 (a). This curve does not contradict the points obtained by the experiment.
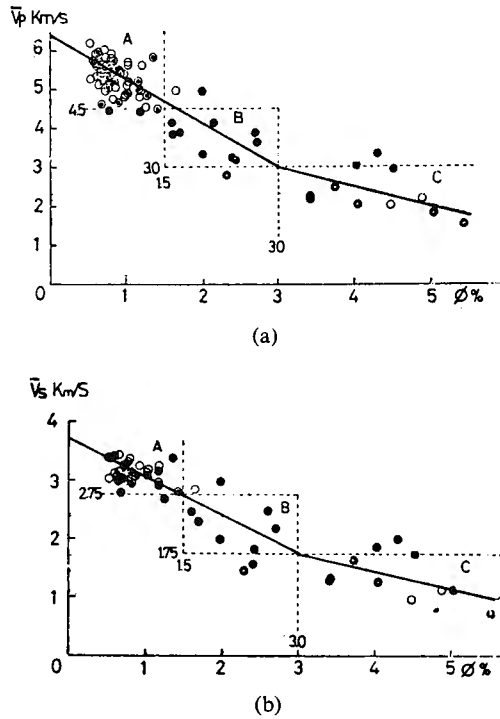
Fig. 9-3. Relation between V_P, V_S and porosity
(laboratory test). (Cited from Kunori et al. [1970])
Symbols, V_P and V_S, in the original paper have
been replaced to symbols, $\overline{V}_P$ and $\overline{V}_S$. Solid lines
are drawn by the author to show representative
tendency of measured values.

c) Gassmann's formulae are applied to the above relation between ϕ and
$\overline{V}_S$, to obtain the relation between ϕ and V_P. Range of V_P values obtained is
3.4—5.7km/s. In sufficient accuracy, $V_S \doteqdot \overline{V}_S$ is hold for the present values of ϕ.
The results evaluated are expressed as $(V_P/V_S; V_P)$ to compare with the author's
relation shown in Fig. 9–2. Both completely coincide each other.

If we trace the preceeding steps reversely, the curve assumed at the first step
(a) can be deduced from the author's relation between V_S and V_P.

d) Even if the pressure effect mentioned in (1) is conducted into the Kunori
and others' relation, variation of V_P/V_S is less than 10%.

(4) Therefore, it is considered that the author's relation expresses rather general
characteristics of granitic rocks. This relation of granitic rocks is also shown in
Fig. 9–4 with that of granular soils deduced from Fig. 9–1. In granular soils, V_P/V_S
at $P=0$ has no meaning, because of $V_S=0$. Boundary between granular soil and
weathered rock seems to be situated at $V_P \doteqdot 2.5$km/s. Distinct characteristics of
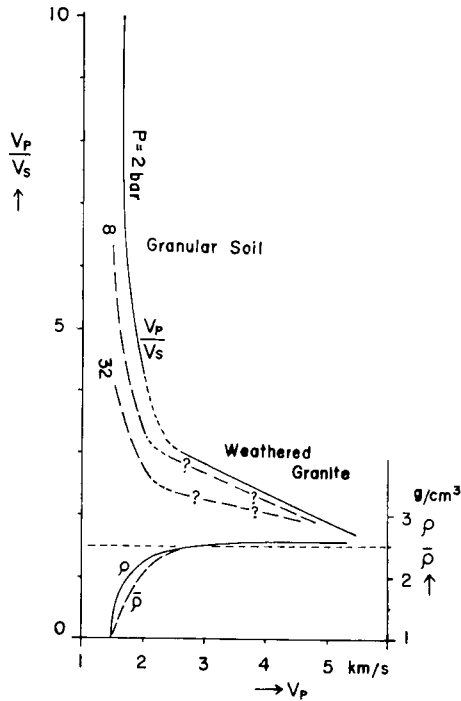velocity are should be noted between both sides of this boundary.

Fig. 9-4. Velocity characteristics of granular soils
and weathered rock.

9-4 Anisotropy

(*1*) Seismic analysis are usually done under the assumption that medium are isotropic. This assumption is approximately correct in many cases. If we define the degree of anisotropy of seismic velocity as ratio of the difference between the maximum and minimum velocity to the minimum velocity, degree of anisotropy in usual sediments is less than about 10%. (As for this, a comment will be attached in (*6*) of 9-4.) However, some kinds of schists have remarkable anisotropy. For example, in black schist of the Sazare mine in Japan, the degree of anisotropy is 28% (Kitsunezaki [1964]). This value may be the maximum one in rock *in situ*.

(*2*) Accompanied with development of seismic experiments in soils, more remarkable anisotropy has been discovered by the author. In some kinds of gravel layer, degree of anisotropy is about 100%. Namely V_P in the horizontal direction is about twice of that in the vertical direction. V_S of SH wave in the horizontal direction is also about twice of V_S in the vertical direction.

This example can be seen in Fig. 5-2 (G2 layer), where, $V_{P//}=1.7$km/s, $V_{P\perp}=0.8$km/s, $V_{P//}/V_{P\perp}=2.1$, $V_{SH//}=0.8$km/s, $V_{S\perp}=0.45$km/s, $V_{SH}/V_{S\perp}=1.8$. Suffix "//" means the horizontal direction (direction parallel to the bedding plane, in strict sense), "⊥" means the vertical (perpendicular to the bedding plane). The

material in G_2 layer of Fig. 5-2 is a mixture of gravel and sand and the maximum diameter of gravel grains is about 20cm. G_1 layer also shows remarkable anisotropic characteristics, where the material is also a mixture of gravel and sand. The maximum diameter of gravel grains is about 5cm.

(3) One of possible explanation for the mechanism of anisotropy has been provided by the theory of alternate bedding. If we suppose that the media consists of two kinds of thin layers, of which elastic constants have been known, we can easily evaluate the resultant seismic constants (anisotropy) by Postma's formulae [1955]. This theory is also introduced in White's text book [1965].

Following his notations, the two kinds of layers are named "1" and "2" respectively. Notations as to each layers are expressed by being attached suffix "1" and "2" respectively. The following notations are defined.

h_1 and h_2 are total thickness of the layers, "1" and "2", in the relevant medium;

$$\eta_1 \equiv \frac{h_1}{h_1 + h_2} \quad , \quad \eta_2 \equiv \frac{h_2}{h_1 + h_2} \; . \tag{9-8}$$

If we assume very extreme properties in the two kinds of layers (element), we can obtain almost all cases of anisotropy. General characteristics of anisotropy of G_2
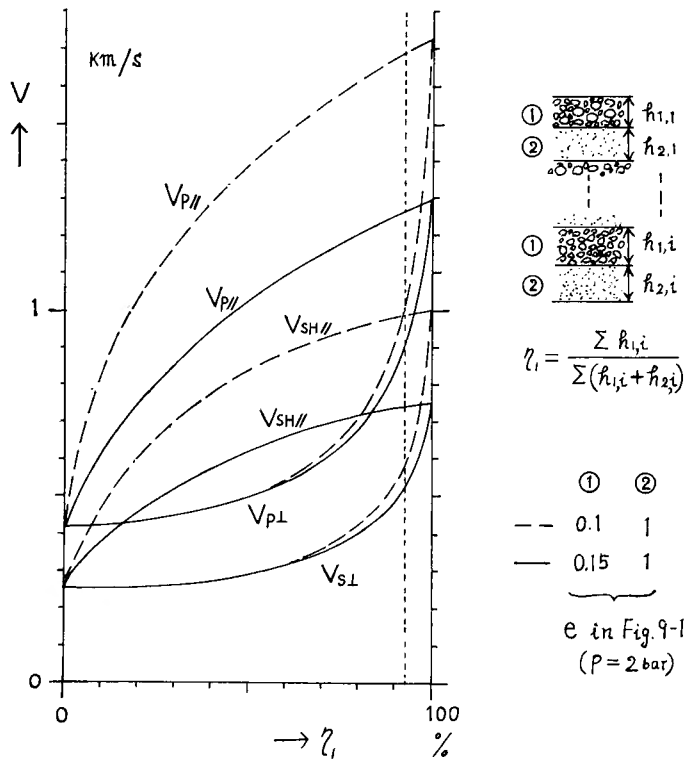

Fig. 9-5. Anisotropy calculated for an alternate bedding model.

layer in Fig. 5–2 also can be explained by this method, at least formally.

We assume that the properties of the two elements correspond to dry granular soils having two different values of e in Fig. 9–1. At first step, we take constants of the elements to be $e_2=0.1$ and $e_1=1.0$, at $P=2$ bar. The calculated results are shown in Fig. 9–5, where η_1 is taken as the variable. If we take certain η_1, we can obtain a model in which velocity ratio of the maximum and the minimum is about two. Main characteristics of the relevant anisotropy is explained by this formally. However, the soil of $e_2=0.1$ seems to be too unusual. Large value of $\overline{V}_{P//}$ requires too large V_P (small e) for one kind of elements.

(4) The case ($e_2=0.1$) assumed in (3) seems to be unnatural. Hence $e_2=0.15$ shall be assumed as possible extreme case. This case is also shown in Fig. 9–5. As tentative assumption, $\eta_1=0.93$ shall be taken, then $\overline{V}_{P//}=1.26$km/s, $\overline{V}_{P\perp}=0.92$ km/s, $\overline{V}_{SH//}=0.74$ km/s, and $\overline{V}_{S\perp}=0.53$ km/s.

In this case resultant e becomes 0.185, which agrees with $e(\fallingdotseq 0.2)$ of the corresponding layer (G2) evaluated by applying $\overline{V}_S=0.6$ km/s $(=\sqrt{\overline{V}_{SH//}\ \overline{V}_{S\perp}}$: the mean velocity) in Fig. 8–6.

(5) In the present layer (Fig. 5–2), gravel grains have flattened shape, and the flattened surface is pararel to the bedding plane. Namely, the shapes are something like ellipsoid rather sphere. Therefore, in the following step, the effect of the shape on anisotropy shall be considered. As for elasticity, granular soils can be approximately explained as a space network of springs. In this network, stiffnesses of each spring, intervals of springs adjoined each other and arrangement of them are key factors to control resultant elastic properties of the whole system. In granular soils, the springs are provided by contacts of grains. The intervals correspond to contact intervals. The arrangement is also arrangement of grains. If those characteristics are not statistically uniform in all direction, anisotropic characteristics may appear in the resultant properties. Alternate bedding is also thought to be anisotropy due to a sort of arrangement.

As to gravel layer having flattened grain, we assume that arrangement is homogeneous and the elongated axis is parallel to bedding plane (horizontal). In this case anisotropic characteristic is due to the intervals. Average of intervals is longer in horizontal direction than in vertical. Namely, number of springs in unit length is less in horizontal direction than in vertical. As far as this characteristic is concerned, the resultant stiffness is larger in horizontal than in vertical. Hence propagation velocity is larger in the horizontal than in the vertical.

However, here is another problem to be considered. If curvatures of the contact planes become larger in horizontal direction accompanied by elongation of shape, each stiffness in horizontal direction becomes smaller. The two effects interfere each other reversely.

(6) In order to evaluate anisotropic characteristics of this type of medium, we shall simplify the condition by assuming the network system as a simple

rectangular-grid system. In this, the springs are arranged only in horizontal and vertical directions, and there is no mechanical interference between them. Ratio of the contact intervals between the two directions are in linear proportion to the diameter ratio. However, the contact stiffness ($\Delta F/\Delta u$ in Table 9-1) is in proportion to 1/3 power of the radius of curvature. Hence, the decrease ratio of the horizontal contact stiffness to the vertical one is less than the increase ratio of the contact intervals in the corresponding directions. By the above reason as a result, the velocity in the horizontal direction becomes higher than the vertical.

The details of the evaluation process are explained in Table 9-1 referring Fig. 9-6. In these table and figure, F is the total force acting on a grain. Shortening radius of sphere (grain), a, in the vertical direction (z) to a/n, a model of the flattend grain (revolutionary ellipsoid) is obtained. u is change of interval of the adjoining grains due to F. P is pressure. ΔF, Δu and ΔP are small variation of F, u and P respectively due to P wave propagation.

In order to evaluate $\Delta F/\Delta u$, the concept of the average radius of curvature of the contact planes is proposed here. This shall be defined as the radius of a sphere which gives the same stiffness as that of the present contact planes. This average radius is shown to be given by the geometrical mean of radii of curvature of the two principal directions with sufficient accuracy after some numerical calculations. In Table 9-1, the values in the line of "average" in the group of the "radius of curvature" mean "the average radius of curvature"

By applying the average radii of curvature instead of a in the expression for $\Delta F/\Delta u$ of the sphere, the corresponding expressions ($\Delta F/\Delta u$) of the revolutionary
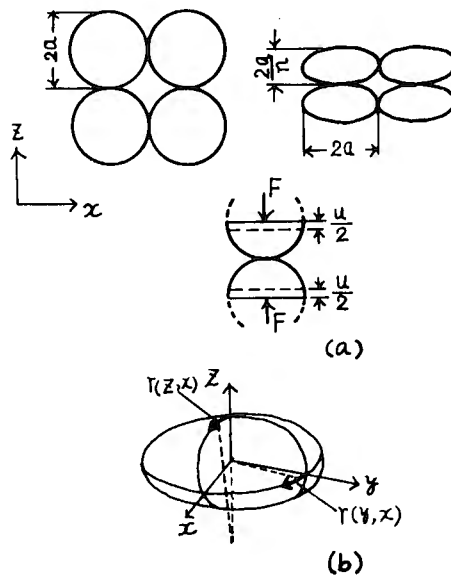

Fig. 9-6. Model of flattened grain packing.

Table 9–1. Evaluation of anisotropy of P wave velocity in the model of Fig. 9–6*

		sphere	revolutionary ellipsoid //		revolutionary ellipsoid ⊥	
axis			x	y	z^*	
radius		a	a	a	a/n	
radius of curvature r				a	na^{***}	x^{**}
			a		na	y
			a/n^2	a/n^2		z
		a	a/n		na	average
$\Delta F/\Delta u$	$\propto$	$(aF)^{1/3}$	$n^{-1/3}(aF)^{1/3}$		$n^{1/3}(aF)^{1/3}$	
F	$\propto$	Pa^2	$n^{-1}Pa^2$		Pa^2	
ΔP	$\propto$	ΔFa^{-2}	$n\Delta Fa^{-2}$		ΔFa^{-2}	
strain ϵ	$\propto$	$a^{-1}\Delta u$	$n^{-1}\Delta u$		$na^{-1}\Delta u$	
$\Delta P/\epsilon$	$\propto$	$P^{1/3}$	$n^{1/3}P^{1/3}$		$n^{-2/3}P^{1/3}$	
$\overline{V}_P$	$\propto$	$P^{1/6}$	$n^{1/6}P^{1/6}$		$n^{-1/3}P^{1/6}$	

Example : radius of curvature r (z^*, x^{**}) (in Fig. 9–6)$=na^{***}$

ellipsoid in vertical ($\perp$) and horizontal (//) directions are obtained. Necessary expression for $\overline{V}_P$ of the revolutionary ellipsoid are evaluated through the processes following the corresponding processes of the sphere (Gassmann [1951b]) which are shown in Table 9–1 for reference.

As the result of the evaluation, the expression for anisotropy is

$$\frac{\overline{V}_{P//}}{\overline{V}_{P\perp}} = \frac{n^{1/6} P_{//}^{1/6}}{n^{-1/3} P_{\perp}^{1/6}} = n^{1/2}\left(\frac{P_{//}}{P_{\perp}}\right)^{1/6}. \qquad (9\text{–}9)$$

In usual soils $P_{//}/P_{\perp}$ is considered to be 1/2. In this case, $(P_{//}/P_{\perp})^{1/6}=0.90$. Based on observation in the field, $n=3$ is assumed,

$$\frac{\overline{V}_{P//}}{\overline{V}_{P\perp}} = 1.73 \times 0.90 = 1.55.$$

The ratio as to $\overline{V}_S$ is also the same as this. Though this evaluation is based on very simplified model, the result may represent approximate characteristics of the real soils.

We assume that the velocities $\overline{V}_P$ and $\overline{V}_S$ in isotropic media of Fig. 9–1 corresponds to the geometrical mean of the maximum velocity and the minimum velocity in anisotropic media.

$$\overline{V}_P = \sqrt{\overline{V}_{P//}\,\overline{V}_{P\perp}}\ ,$$

$$\overline{V}_P = \overline{V}_{P//}\Big/\sqrt{\frac{\overline{V}_{P//}}{\overline{V}_{P\perp}}} = \overline{V}_{P\perp}\sqrt{\frac{\overline{V}_{P//}}{\overline{V}_{P\perp}}} \qquad (9\text{–}10)$$

---

* Some errors involved in the author's previous report [1970b] have been corrected in this table.

In the above numerical example,

$$\overline{V}_{P//} = 1.25 \, V_P \, , \qquad \overline{V}_{P\perp} = \overline{V}_P/1.25. \qquad (9\text{--}11)$$

(7)   After all, anyone of two types of the models mentioned above is insufficient to explain the velocity anisotropies observed. However, considering coexistance of these two mechanisms where the effects of them are assumed to be mutually multiplied, the observed anisotropies seem to be explained. The velocity ratios of Eq. (9–11) are multiplied to the ratios of the velocities obtained in (4) holding the average velocities $\overline{V} = \sqrt{\overline{V}_{//}\overline{V}_{\perp}}$ as those in (4);

$$\overline{V}_{P//} = 1.57 \text{ km/s}$$
$$\overline{V}_{P\perp} = 0.74 \text{ km/s}$$
$$\overline{V}_{sH//} = 0.92 \text{ km/s}$$
$$\overline{V}_{S\perp} = 0.42 \text{ km/s}.$$

Combination of such two kinds of mechanisms may provide the most possible explanation of anisotropy in this field under discussion.

By observation in sight, alternation in this layer are not so clear. According to the above example, a little sand ($e_2 = 7\%$) affects remarkably on resultant anisotropy. Most part of such sand may lie horizontally between gravel grains, rather in irregular form.

(8)   There is a problem on the flattened grain model mentioned above. In this model, contact plane was assumed to have round curvature. Hence the exponent of pressure applied in the expression for pressure depending of velocities is 1/6. This is based on Hertz's theory (Timoshenko [1951]). However, Fig. 9–1 is evaluated based on Hardin's experiment, in which exponent of pressure is 1/4. This discrepancy is neglected in the above discussion.

(9)   If granular soils are saturated by water, degree of anisotropy of V_P becomes remarkably smaller, though the difference does not occur as to V_S. This is one of reasons why degree of anisotropy is small in usual sediment where only V_P has been measured under water-saturated condition in almost all cases. By this reason, we must be careful to discuss the velocity characteristics, especially in S wave. In general, knowledges obtained by measurement of V_P in deeper places are apt to be directly applied for evaluation of characteristics of V_S in any places, and of V_P in shallower places. This will conduct false conclusion.

(10)   As an example mentioned in (9), evaluated velocities in water-saturated condition will be shown as for G2 layer in Fig. 5–2. The following values shall be assumed in addition to the values in (2).

$$\overline{\rho} = 2.2 \, g/cm^3 \, , \qquad e = 0.20$$

This value of e is obtained by giving $V_S = 0.6$km/sec ($= \sqrt{V_{S\,H//} \, V_{S\perp}}$) in Fig. 8–6.

The following values are obtained by applying Gassmann's formulae [1951a];

$$V_{P//} = 2.52 - 2.42 \text{ km/s}, \qquad V_{P\perp} = 2.22 - 2.16 \text{ km/s},$$
$$V_{SH//} = 0.77 \text{ km/s}, \qquad V_{S\perp} = 0.43 \text{ km/s},$$
$$V_{P//}/V_{P\perp} = 1.14 - 1.12, \quad (\ddot{V}_{P//}/\overline{V}_{P\perp} = 2.13!),$$
$$V_{SH//}/V_{S\perp} = \overline{V}_{SH//}/\overline{V}_{S\perp} = 1.78.$$

The range of the values means variation due to the allowable range of another constant, which can not be given from the velocities in (2). (Complete number of elastic constant of transversely isotropic media is five. Measured one in (2) is four.)

10. Problems relating to engineering seismology

(1) During earthquake, aspects of vibration on the ground surface are effected by the under-ground structure below the site. Seismic waves generated by an earthquake are incident upwards to some regions of the earth surface. The waves meet low velocity layers near the ground. The aspects of waves are strongly modified in these near-surface layers by reflection and refractions. In this case, propagation direction in the surface layers is almost vertical because of its low velocity characteristics. Hence, horizontal motion on the ground surface, which is considered to be main cause of structure destroying, is provided by the S wave. For this reason characteristics of the S wave in the surface layer has important meaning in engineering seismology. The fact mentioned above is well known, and attentions have been concentrated to survey the above characteristics.

(2) In general, velocity distribution of earth surface can be understood by being devided into two groups as to depth.

a) If we start from the ground surface at fitst, we find very low velocity soils in the near-surface. This can be understood as natural also by considering the pressure effect discussed in Section 9. And there, velocities usually show remarkable variation in relatively small scale. This layer shall be called shallower surface layer (named I). Layer I usually corresponds to alluvium, and sometimes to upper part of diluvium.

b) Up to 10—100 m, we enter higher velocity region, where tendency of velocity variation may be relatively gentle. For example, depth of 100 m usually corresponds to more than about 10 bar in effective pressure. From Fig. 9–2, it is difficult to consider velocity less than 300 m/s. Void ratio also becomes higher by effects due to longer geological history. This layer shall be called deeper surface layer (named II). Velocity in this layer becomes gradually higher as the whole tendency. Velocities of rock in upper part of the crust below Layer II are almost constant.

$$V_P \fallingdotseq 5.5 \text{ km/s}$$
$$V_S \fallingdotseq 3.0 \text{ km/s}$$

There is a large velocity difference between Layer II and deeper rock. The velocity ratio of the latter to shallower part of Layer II is about 5-10. The velocity distribution in Layer II with depth and space provides problems to be considered for the present purpose.

As deeper boundary of Layer II, the depth, where V_S reaches practically constant value, shall be taken. Layer II usually corresponds to diluvium and sometimes upper part of tertiary.

(3) For convenience sake, we regard the effects of the surface layers as filters. Hence, there are two kinds of filter, I and II corresponding to two kinds of layers. Layer I gives direct effect of vibration on ground surface. Attention has been also concentrated to this layer. Explanation of wave modification in this layer is usually provided by multiple reflection theory (Kanai [1953] [1970] for example). Effective period of Filter I is relatively shorter, usually less than 0.5 sec., which is also within the range of resonance period of usual structures. And in Layer I, the ground itself is also fractured due to earthquake sometimes.

The characteristics of Filter II is somewhat different from I. Filter II has two kinds of effect.

a) The resonance period of Layer II is longer than I. Hence this affects the component of longer period of earthquake waves.

High storyed buildings have been constructed recently in Japan. They have the resonance period of several seconds, which is about ten times of usual low storeyed building. Effective thickness of Layer II to give such resonance period is more than ten times of that of I.

For example, we assume $V_S = 0.6$ *km/sec*, resonance period $T=4$ *sec*. The effective thickness H corresponding to this is $H = V_S T/4 = 0.6$ *km*. By the above reason survey of II is also important.

b) Seismic waves refract, when they are incident to a layer with different velocity. Ray density of seismic waves may be made dense or rare, under certain conditions. A sort of lens effect can be expected in such particular structures. Certain curvature of lower boundary of Layer II and certain special velocity distribution in Layer II may provide such conditions. For the reason mentioned above, sufficient attention should be paid also to syncline structures.

Too long wavelength comparable with scale of structure can not bring such lens effect. Hence this phenomena have effect on seismic waves with rather shorter period.

Though existance of such effect has not been acertainecd really, it may be sufficiently possible in particular conditions.

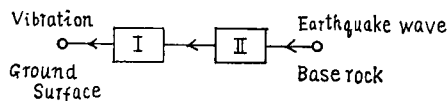After all, effect of surface layer should be investigated as series of two filters,

Fig. 10–1. Surface effects on earthquake waves.

as shown in Fig. 10–1. The present interest focuses on the problem in relation with the S wave. These problems will be discussed in the following.

(4) The S wave survey of Layer Ⅰ shall be discussed here. In this case, depth necessary to be surveyed is usually less than 50 m. The whole methods for S wave logging discussed in Section 7 and 8 are available for this purpose. Especially, a combination of a borehole geophone and a source set on the ground surface can be effectively applied.

In shallower layer, regional variation of wave characteristics is expected large, and S wave logging should be done at each site of interest.

In big earthquakes, strain amplitude of vibration becomes very large, and hence values of V_s in real earthquakes may be obtained by modifying values of V_s measured by logging technique. This is the important problem for engineering earthquakes. However, this does not decrease the significance of S wave logging in real media. The values measured by this method provide standard properties of the ground. Based on other investigation, those values should be corrected by mutiplying certain practical coefficients, to use them for evaluation of earthquake effects.

(5) As to Layer Ⅱ, the whole aspect of S wave logging must be different from that in Ⅰ.

Principally, deep boreholes are needed. The logging probe consisting of geophones and the source is favourable for this purpose. This method has not been completed. Development of this instrument is necessary.

In order to avoid technical and economical difficulties of the above logging, indirect method for S wave logging also should be available, with well combination of the direct method.

As to Layer Ⅱ, there is no need of such a detail survey as Layer Ⅰ. Larger scale characteristics become more important. Since we can not expect to have many deeper boreholes, geological considerations must be stressed. From knowledges of relatively shallower depth and restricted data of deeper depth, we must infer the wide scale characteristics of region.

This work should be carried out as one branch of regional studies having wide aspects, with well combination of geology and water resource study etc., for example. From the above point of view, data of water-wells and boring surveys should be collected under the certain standards as routine works. Indirect methods have important meaning in this aspect.

Seismic prospecting (P wave) of relatively large scale provides necessary knowledge as to base rock. Such survey was carried out by the author and others [1971]. Other methods of geophysical prospecting and also observation of microtremor (Kubotera, et al. [1970]) may have sufficient meaning. S wave characteristics must be attached to the structure explored by the variable methods. Therefore, a well concerted attack from many sides is very important.

11.   Conclusion

In this paper, main aspects of the author's studies on the S wave and of the related problems are presented in systematic form, stressing on his recent works and fundamental problems.

1)   Observation by geophones consisting of three component detectors (velocity type) provides the fundamental means for detection and identification of S wave, being supported with supplementary use of hydrophones.

2)   Higher frequency characteristics of the detectors must be noted for detailed and exact observation of seismic waves of short period.   Installation condition of the geophone also has the effect on the higher frequency characteristics through the whole observation system.

3)   The S wave can be relatively easily generated by an explosion and an impulsion.   It, however, needs some devices to generate the S wave free from interference of other kinds of seismic waves.

4)   The whole aspects of seismic waves, as to generation, attenuation and propagation, are systematically understood, by scaling factors of length with their ratio to wavelength.

5)   The whole aspects of the S wave survey strongly depend on conditions of each field.   Some devices are usually necessary to get successful results.   Availability of the various souce, including wave conversion also, must be paid attention.

6)   Velocity variation of fractured (weathered) rock (granitic) and granular soils are governed mainly by void ratio and pressure.   However, both show different characteristics as to the relation between V_P/V_S and V_P.   A boundary between them exists at $V_P \fallingdotseq 2.5$ km/sec.

7)   Many kinds of direct and indirect methods for S wave logging are discussed in Section **7**, **8**, **9** and **10**.   In shallower depth, use of a borehole geophone (with the source on the ground surface) is most available in usual field condition from practical point of view.

8)   In deeper depth, a special logging probe consisting of the detectors and the source must be inserted into a borehole.

9)   The indirect method for S wave logging provides supplementary means for wide regional survey.

10)   As to engineering seismology, characteristics of relatively deeper structures should be paid attention to.   Regarding the S wave survey for this purpose, a well concerted attacks in necessary.   For example, they are direct and indirect S wave logging, geological study, water resource research, many kinds of geophysical prospecting and observation of microtremor.

Acknowledgement

References

Archie, G. E., 1942; The electrical resistivity log as an aid determining some reservoir characteristics, AIME, **146**, 54.

Biot, M. A., 1952; Propagation of elastic waves in a cylindrical bore containing a fluid, J. Appl. Phys., **23**, 997–1005.

Case, K. M., and Colwell, J. F., 1967; Elastic waves radiated by a small source, Geophys., **32**, No. 1, 52–59.

Doboku-buttan-kenkyu-kai [Research Group of Geophysical Prospecting for Civil Engineering], 1970; On shear wavevelocity, Butsuri-tanko, **23**, 179–162 (in Japanese).

Ewing, W. M., W. S. Jardetzky and P. Frank, 1957; Elastic Waves in Layered Media, McGraw-Hill Book Co., New York.

Gassmann, F., 1951 a; Uber die Elastizität poröser Medien, Vierteljahrsschr. Naturforsch. Ges. Zurich, **96**, 1–23.

Gassmann, F., 1951 b; Elastic waves through a packing of spheres, Geophys, **16**, 673–685.

Hagiwara, Y., 1958; A rotation seismometer, Zishin, **11**, 141–144 (in Japanese).

Halperin, E. I., and A. V. Frolova, 1961; Three-component seismic observation in boreholes, II, Bull. Acad. Sci. USSR, Geophys. Ser. (English Transl.), 644–653.

Hardin, B. O. and F. E. Richart, 1963; Elastic wave velocities in granular soils, Journal of the Soil Mechanics and Foundation Division, ASCE. **89**, 33–65.

Hardin, B. O. and W. Block, 1968; Vibration modulus of normally consolidated clay, Jour. of the Soil Mech. and Found. Divis., ASCE. **94**, 353–369.

Heelan, P. A., 1953; Radiation from a cylindrical source of finite length, Geophys., **18**, 685–696.

Honsho, S., 1966; Velocity change of sedimentary rocks due to uniaxial pressure, Butsuri-tanko, **19**, 87–85.

Jolly, R. N., 1953; Deep-hole geophone study in Garvin County, Oklahoma, Geophys, **18**, 662–670.

Jolly, R. N., 1956; Investigation of shear waves, Geophys., **21**, 905–938.

Kanai, K., 1952; Relation between the nature of surface layer and the amplitude of earthquake motion, I, Bull. Earthq. Res. Inst., **30**, 31–37.

Kanai, K., 1953; Relation between the nature of surface layer and the amplitude of earthquake motion, II, Bull. Earthq. Res. Inst., **31**, 219–226.

Kanai, K. and S. Yoshizawa, 1953; Relation between the nature of surface layer and the amplitude of earthquake motion, III, Bull. Earthq. Res. Inst., **31**, 275–279.

Kanai, K., 1970; Engineering Seismology, Kyoritsu-shuppan Co., Tokyo (in Japanese).

Kisslinger, C., Mateker, E. J. and T. V. Mc Evilly, 1961; SH motions from explosions in soil, Jour. Geophys. Res., **66**, 3487–3496.

Kitsunezaki, C., 1960 a; Study on high frequency seismic prospecting (1), Butsuri-tanko, **13**, 102–107, 137–146 (in Japanese).

Kitsunezaki, C., 1960 b; Study on high frequency seismic prospecting (2), Butsuri-tanko, **13**, 185–193 (in Japanese).

Kitsunezaki, C., and H. Koseki, 1960c; New pick-up for high frequency prospecting, Butsuri-tanko, **13**, 244–245 (in Japanese).

Kitsunezaki, C., 1961; Study on high frequency seismic prospecting (3), Butsuri-tanko, **14**, 125–129 (in Japanese).

Kitsunezaki, C., 1963; High frequency seismic prospecting, Geophysical Papers Dedicated to Prof. K. Sassa, Geophys. Inst., Kyoto Univ., 179–185.

Kitsunezaki, C., 1964; Determination of seismic anisotropy of metamorphic rocks in natural conditions, Special Contribution, Geophys. Inst., Kyoto Univ., **4**, 83–90.

Kitsunezaki, C., and N. Goto, 1964; On the determination of geophone characteristics by "step force method", Butsuri-tanko, **17**, 166–175 (in Japanese).

Kitsunezaki, C., 1965; *Insitu* determination of variation of Poisson's ratio in granite accompanied by weathering effect and its significance in engineering projects, Bull. Disast. Prev. Res. Inst., Kyoto Univ., **15**, 19–41.

Kitsunezaki, C., 1967 a; Observation of S wave by the special borehole geophone (1), Butsuri-tanko, **20**, 1–15 (in Japanese).

Kitsunezaki, C., 1967 b; Observation of S wave by the special borehole geophone (2), Butsuri-tanko, **20**, 47–57 (in Japanese).

Kitsunezaki, C., 1967 c; Calibration of higher frequency characteristics of geophone, Special Contributions, Geophys. Inst., Kyoto Univ., **7**, 181–199.

Kitsunezaki, C., 1967 d; Expression for reflection and transmission coefficient, Butsuri-tanko, **20**, 161–164 (in Japanese).

Kitsunezaki, C., 1968; Rigidity logging utilizing tube wave, Butsuri-tanko, **21**, 199–210 (in Japanese).

Kitsunezaki, C., and N. Goto, 1969; Velocity measurement of shear wave by using clamped borehole geophone, Annuals, Disast. Prev. Res. Inst., Kyoto Univ., **12A**, 191–204 (in Japanese).

Kitsunezaki, C., 1970a; Underground structure and seismic wave velocities in Uji campus of Kyoto University, Annuals, Disast. Prev. Res. Inst., Kyoto Univ., **13A**, 175–195 (in Japanese).

Kitsunezaki, C., 1970b; Some problems on S wave logging, Contribution to the Seismic Exploration Group of Japan, **54**, 3–50 (in Japanese).

Kitsunezaki, C., 1970c; Solenoid-hammer as electro-mechanical transducer used for seismic source (1), Butsuri-tanko, **23**, 86–96 (in Japanese).

Kitsunezaki, C., 1971a; Theory of electromagnetic seismograph (7), Butsuri-tanko, **24**, 143–158 (in Japanese).

Kitsunezaki, C., 1971b; Theory of electromagnetic seismograph (8), Butsuri-tanko, **24**, 198–205 (in Japanese).

Kitsunezaki, C., N. Goto and Y. Iwasaki, 1971; Underground structure of the southern part of the Kyoto Basin obtained from seismic exploration and some related problems of earthquake engineering, Annuals, Disast. Prev. Res. Inst., Kyoto Univ. **14A**, 203–215, (in Japanese).

Kobayashi, N., 1959; A method of determining of the underground structure by means of SH wave, Zisin, **12**, 19–24 (in Japanese).

Kubotera, A., and M. Otsuka, 1970; Nature of no-volcanic microtremor observed on the Aso Caldera, Jour. of Phys. of the Earth, **18**, 115–124.

Kunori, S., M. Abe, and T. Saito, 1970; Study of weathering of Granitic rocks, Butsuti-tanko, **24**, 6–17 (in Japanese).

Lastrico, R. M., 1970; Effects of site and propagation path on recorded strong earthquake

motion, Doctor Thesis, School of Enq. and Appl. Sci., Univ. of Calif., Los Angels.

Linsser, H., 1955; Anwendungsmöglichkeiten transversalen Wellen in der Untertage-seismik, Zeit. F. Geophys., 20, 150–159.

Love, A. E. H., 1952; A treatise on the mathematical theory of elasticity, Cambridge University Press.

Matsushima, S., 1960; Variation of elastic wave velocities of rocks in the process of deformation and fracture under high pressure, Bull. Disast. Prev. Res. Inst., Kyoto Univ., 32, 1–8.

Macdonald, F. J., A. Angona, R. L. Mills, R. L. Sengbush, R. G. Von Nostrand, and J. E. White, 1958; Attenuation of shear and compressional waves in Pierre Shale, Geophys. 23, 421–439.

Nakano, S., and Y. Okano, 1960; Mechanism of explosive source with cylindrical shape, Zishin, 22, 328–346 (in Japanese).

Nasu, N., T. Hagiwara, and S. Omote, 1936; Studies on the propagation of the artificial earthquake waves through superficial soil or sand layers and the elasticity of soil and sand, Bull. Earthq. Res. Inst., 14, 560–581 (in Japanese).

Ohta, Y., 1968; S ha no hassei to sono riyo [Generation and application of S wave], Butsuri-tanko, 20th Anniversary, 227–238 (in Japanese).

Postma, G. W., 1955; Wave propagation in a stratified medium, Geophys. 20, 780–806.

Seed, B., 1969; The influence of local soil condition on earthquake damage, Preprint, Soil Dynamic Special Conf., Mexico (Aug. 1969).

Shima, E. and Y. Ohta, 1967; Experimental study on generation and propagation of S waves I; Designing SH-wave generator and its field tests, Bull. Earthq. Res. Inst., 45, 19–32.

Shima, E., Y. Ohta, M. Yanagisawa, K. Kudo, and H. Kawasumi, 1968; S wave velocities of subsoil layers in Tokyo (3), Bull. Earthq. Res. Inst., 46, 1301–1312.

Shulumberger Well Survey Corp., 1949; Resistivity departure curves, Schlumberger Document No. 3.

Tazime, K., and N. Den, 1965; A test production of a rotation seismometer for seismic prospecting, Geophys. Bull. of Hokkaido Univ., 14, 95–104 (in Japanese).

Telzaghi, K. and R. B. Peck, 1948; Soil mechanics in Engineering Practice, John Wilely and Sons, New York.

Timoshenko, S., 1951; Theory of elasticity, McGraw-Hill Book Co., New York.

White, J. E., and R. L. Sengbush, 1953; Velocity measurements in near-surface formations, Geophys, 18, 54–69.

White, J. E., 1962; Elastic waves along cylindrical bore, Geophys., 27, 327–333.

White, J. E., and R. L. Sengbush, 1963; Shear waves from explosive sources, Geophys, 28, 1001–1019.

White, J. E., 1965; Seismic waves, McGraw-Hill Book Co., New York.

Yamaguchi, K., 1963; Sakusen no Denki-Kensō [Electrical logging in well], Shyōkō-dō, Tokyo (in Japanese).

Yoshikawa, S. and C. Kitsunezaki, 1964; On the application of seismic prospecting in engineering projects, Annuals, Disast. Prev. Res. Inst., Kyoto Univ., 7, 39–49.

Yoshikawa, S., and K. Zako, 1970; Jishin-tansa no oyo to Jisshi-rei [Application of seismic prospecting and example of its practice], Lecture Text, Kansai Branch of Japan Soc. of Civil Eng (in Japanese).

Yoshimura, M., H. Fumoto, and T. Imai, 1970; Kayaku-bakuhatsu ni yotte shojita "S" ha, [S wave generated by an explosion] Pre-print for Lecture at Autumn Meeting, 1970, Seismological Soc., Japan (in Japanese).